Regime switching in stochastic models of commodity prices: An application to an optimal tree harvesting problem

Shan Chen[1] Margaret Insley[2]

August 28, 2008

[1]Shan Chen is a PhD Student in the Department of Economics, University of Waterloo, Waterloo, Ontario, N2L 3G1. email: s32chen@artsmail.uwaterloo.ca

[2]Margaret Insley is an Associate Professor in the Department of Economics, University of Waterloo, Waterloo, Ontario, Canada, N2L 3G1. email: minsley@uwaterloo.ca

Abstract

Regime switching in stochastic models of commodity prices: An application to the optimal tree harvesting problem

This paper investigates a regime switching model of stochastic lumber prices in the context of an optimal tree harvesting problem. Using lumber derivatives prices, two lumber price models are calibrated: a regime switching model and a single regime model. In the regime switching model, the lumber price can be in one of two regimes in which different mean reverting price processes prevail. An optimal tree harvesting problem is specified in terms of a linear complementarity problem which is solved using a fully implicit finite difference, fully-coupled, numerical approach. The land value and critical harvesting prices are found to be significantly different depending on which price model is used. The regime switching model shows promise as a parsimonious model of timber prices that can be incorporated into forestry investment problems.

Keywords: optimal tree harvesting, regime switching, calibration, lumber derivatives prices, fully implicit finite difference approach

Running Title: Regime switching prices and optimal tree harvesting

1 Introduction

The modelling of optimal tree harvesting and the valuation of land devoted to commercial timber harvesting is an active research area in the academic literature. A more than thirty-year-long strand of this literature emphasizes the importance of valuing managerial flexibility in the context of irreversible harvesting decisions when forest product prices are volatile relative to harvesting costs.[1] An ongoing challenge is how best to model the dynamics of timber prices in determining optimal harvesting strategies and in estimating the value of forested lands. Over the past two decades some researchers have modeled price as a stochastic differential equation (see Thomson (1992); Plantinga (1998); Morck et al. (1989); Clarke and Reed (1989) for example). Another approach is to model stand value (price of wood times quantity of wood), as a stochastic differential equation, such as in Alvarez and Koskela (2007) and Alvarez and Koskela (2005).

The model chosen to describe timber prices can have a significant effect on optimal harvesting decisions and land valuation. The issue is therefore of importance to forest management, whether on publicly or privately owned land. There has been a trend over the last two decades to view commercial timber lands as a suitable asset to diversify the portfolios of large investors. Institutional investors in the United States have significantly increased their holdings of timberlands, giving an added motivation for a better understanding of timber price dynamics and investment valuation.[2]

Several specifications have been proposed in the literature for modeling stochastic lumber prices, including Geometric Brownian Motion (GBM), Mean Reversion and Jump processes. A number of researchers have solved optimal tree harvesting problems analytically, assuming prices follow GBM.[3] Some researchers have found that mean reversion rather than GBM provides a better characterization of lumber prices (Brazee et al. (1999)). For commodities in general, it has been argued that mean reversion in price makes sense intuitively since any significant upturn in price will bring on additional supplies. The assumption of a price process other than GBM generally requires numerical solution of an optimal tree harvesting problem. This can present significant challenges particularly if the researcher chooses to model the growing forest stand in a realistic fashion over multiple rotations or cutting cycles.

Unfortunately it is difficult to conclude definitively which price process is most appropriate for any particular commodity. As is noted in Insley and Rollins (2005) many different statistical tests exist, but none has been shown to be uniformly most powerful. Saphores et al. (2002) find evidence of jumps in Pacific North West stumpage prices in the U.S. and demonstrate at the stand level that ignoring jumps can lead to significantly suboptimal harvesting decisions for old growth timber. A recent insight in the literature suggests that instead of modeling jumps in commodity prices, we may consider regime switching models, initially proposed by Hamilton (1989), to better capture the main characteristics of lumber price.

Using a regime switching model, the observed stochastic behavior of a specific time series

[1] Hool (1966); Lembersky and Johnson (1975) are examples of some of the earlier literature.

[2] See Global Institute of Sustainable Forestry (2002) and Caulfield and Newman (1999) for a discussion of this shift in ownership.

[3] Examples are Clarke and Reed (1989) and Yin and Newman (1997).

is assumed to be comprised of several separate regimes or states. For each regime or state, one can define a separate and independent underlying stochastic process. The switching mechanism between each regime is typically assumed to be governed by an unknown random variable that follows a Markov chain.[4] Various factors may contribute to the random shift between regimes, such as changes in government policies and weather conditions.

Several authors, building on the seminal work of Hamilton (1989), have modeled commodity prices by allowing parameters of the process to change over time driven by a Markov state variable. For example, Deng (2000), de Jong (2005), Chen and Forsyth (2008) all examine empirical models of regime switching in commodity prices (electricity or natural gas prices) and have shown promising results for their empirical applications.

In this paper we investigate whether a regime switching model is a good alternative for modelling stochastic timber prices. For simplicity we assume the existence of two states or regimes. In line with Chen and Forsyth (2008), we calibrate a regime switching model with timber price as the single stochastic factor which follows a different mean reverting process in each of two regimes. We compare this model (denoted the RSMR model) with a single regime mean reverting model (denoted the traditional mean reverting, or TMR, model) which has been used previously in the literature. For parameter calibration, these two models are expressed in the risk-neutral world and the corresponding parameters are calibrated using the prices of traded lumber derivatives, i.e. lumber futures and options on lumber futures. A benefit of calibrating model parameters in this way is that the parameters obtained are risk adjusted so that a forest investment can be valued using the risk-free interest rate, with no need to estimate a market price of risk.

In the second part of the paper we use the calibrated RSMR and TMR models to solve an optimal harvesting problem. The optimal choice of harvesting date for an even-aged stand of trees and the value of the option to harvest are modeled as a linear complementarity problem which is solved numerically using a fully implicit finite difference method. The approach is similar to that used in Insley and Lei (2007), except that the model must accommodate the different regimes. We use the same cost and timber yield estimates as in Insley and Lei (2007) and hence we are able to compare results. In Insley and Lei (2007) parameter estimates of the price process were obtained through ordinary least squares on historical lumber price data only.

This paper makes a methodological contribution to the literature. It demonstrates the numerical solution of a dynamic optimization problem in a natural resources context under the assumption of a regime switching stochastic state variable. In the future it is hoped that this methodology may be usefully applied to other types of natural resource investment problems, which are often sufficiently complex that closed-form solutions are unavailable. The paper also makes an empirical contribution in the investigation of the dynamics of lumber prices. To our knowledge the parameterization of stochastic lumber price models using lumber derivatives prices has not been done previously in the literature. Although we are limited by the short maturity dates of traded lumber futures, we find that the RSMR model shows promise as a parsimonious model of timber prices that can be incorporated into problems of forestry investment valuation using standard numerical solutions techniques. In

[4] A Markov chain has the property that, given the present, the future is conditionally independent of the past.

our concluding section we discuss how this and other limitations of the current paper point toward avenues for future research.

The remainder of the paper will be organized as follows. Section 2 presents a brief literature review. Section 3 provides descriptive statistics and preliminary tests on a lumber price time series. Section 4 specifies the lumber price models that will be used in our analysis and details the methodology for calibrating the parameters of these models. Section 5 provides the results of the calibration. Section 6 uses the regime switching and single regime price models to solve for the optimal harvesting time and land value in a tree harvesting problem. Section 7 provides some concluding comments.

2 Modeling commodity prices: An overview of selected literature

Stochastic models of commodity prices play a central role for commodity-related risk management and asset valuation. As noted in Schwartz (1997), earlier research into valuing investments contingent on stochastic commodity prices generally adopted an assumption of geometric Brownian motion (GBM), $dP = aPdt + bPdz$, where P denotes commodity prices, a and b are constant, dz is a standard Winner process. This allowed the procedures developed for valuing financial options to be easily extended to valuing commodity based contingent claims.

Schwartz (1997) and Baker et al. (1998), among other, have emphasized the inadequacy of using GBM to model commodity prices. Under GBM the expected price level grows exponentially without bound. In contrast there is evidence that the real prices of many natural resource-based commodities have shown little upward trend. This is explained by the presence of substitutes as well as improvements in technology to harvest or extract a resource. In the literature on optimal tree harvesting, early papers adopting the GBM assumption include Reed and Clarke (1990), Clarke and Reed (1989), Yin and Newman (1995), and Morck et al. (1989).

We can also gain insight into the appropriateness of a GBM model for commodity prices by observing futures prices. The current price of a futures contract at time t with maturity T, denoted $F(t,T)$ equals the risk neutral expectation of the spot price, $P(t)$, that will prevail at time T.[5]

$$F(t,T) = E^Q[P(T)|P(t)] = P(t)e^{(r-\delta)(T-t)} \tag{1}$$

where r is the risk free rate δ represents the convenience yield, and E^Q represents the expectation in the risk neutral world or under the "Q-measure". If P follows GBM,it can be demonstrated using Ito's lemma that the futures price will also follow GBM, and both P and F will have the same (constant) volatility. However, for most commodities, the volatility of futures prices decreases with maturity,so that the single factor lognormal model such as GBM is not consistent with reality (Pilipovic, 2007, page 233-234).

[5] In other words, the futures price should be equal to the expected spot price after adjusting for a risk premium or discount. See Geman (2005) for a discussion of futures prices and the risk neutral dynamics of commodity prices

It is not unreasonable to expect that the workings of supply and demand will result in commodity prices that exhibit some sort of mean reversion. There is also empirical research that supports this claim. For example Bessembinder et al. (1995) find support for mean-reversion in commodity prices by comparing the sensitivity of long-maturity futures prices to changes in spot prices.

If mean reversion is accepted as a desirable property, there are several possible stochastic models to choose from which incorporate mean reversion. The simplest mean reverting process, the Ornstein-Uhlenbeck process, is given as

$$dP = \alpha(K - P)dt + \sigma dz. \tag{2}$$

α is a constant and referred to as the speed of mean reversion. K represents the (constant) long run equilibrium price that P will tend towards. The instantaneous volatility, σ, is also constant and dz is the increment of a Wiener process.

In a common variation of the Ornstein-Uhlenbeck process, the conditional variance of P depends on the level of P, thereby preventing P from becoming negative:

$$dP = \alpha(K - P)dt + \sigma P dz. \tag{3}$$

This process is adopted in Insley and Rollins (2005) and Insley and Lei (2007) to represent lumber prices in an optimal tree harvesting problem. Other optimal harvesting papers to adopt variations on these mean reverting processes include Plantinga (1998) and Gong (1999). Mean reverting processes have also been used in modeling prices for oil, electricity, copper, and other minerals (see Cortazar and Schwartz (1994), Dixit and Pindyck (1994), Pilipovic (2007), Smith and McCardle (1998) and Lucia and Schwartz (2002) for example).

The simple mean reverting models of Equations (2) and (3), while an improvement over GBM, are not entirely satisfactory. It can be shown that under these models the implied volatility of futures prices decreases with maturity, which is a desirable property for modelling commodity prices. However volatility tends to zero for very long maturities, which is not consistent with what is observed in practice. In addition these models presume a constant long run equilibrium price (K), when in reality K may be better characterized as a stochastic variable. Schwartz and Smith (2000) propose a two-factor model in which the equilibrium price level is assumed to evolve according to GBM and the short-term deviations are expected to revert toward zero following an Ornstein-Uhlenbeck process. In another variation, a commodity's convenience yield is modelled as additional stochastic factor which is assumed to follow a MR process. Schwartz (1997) also develops a three-factor model with stochastic price, convenience yield and interest rate. Alternative versions of multi-factor models can be derived through variation of a number of dimensions. However the more factors incorporated into the model, the more complicated is the solution of the resulting partial differential equation that describes the value of contingent claims on the commodity.

Another consideration that may be important in modeling commodity prices is the presence of jumps. Barz and Johnson (1998) suggest the inadequacy of the GBM and MR specification in modeling electricity spot prices and offer a broad class of stochastic models which combine a mean-reverting process with a single jump. Kaminski (1997) points out the need to introduce jumps and stochastic volatility in modeling electricity prices. As noted in the Introduction, Saphores et al. (2002) allow for the presence of jumps as well as ARCH effects in modelling stumpage prices for lumber from old growth forests in the Pacific northwest. They also investigate the empirical impact of jumps by assuming that stumpage prices for old-growth forest follow a GBM with jumps, and show that ignoring jumps may lead to significantly suboptimal decisions to harvest timber.

In devising better models for commodity prices we are faced with a tradeoff between increased realism through the addition of more stochastic factors, jumps, etc., and the added complexity and difficulty of solving for the value of related contingent claims. The optimal tree harvesting problem has the further complication that the asset (a stand of trees) is growing and being harvested over multiple rotations. The timing of harvest and hence the age of the stand depend on price, so that stand age is also a stochastic factor. It is desirable to find an approach to modeling timber prices which, while adequately rich, still allows for the solution of the related contingent claim using standard approaches. It is towards this end that we investigate a regime switching model. The regime switching model with two regimes can readily be solved with a finite difference numerical approach.

Jumps in commodity prices are often driven by discrete events such as weather, disease, or economic booms and busts which may persist for months or years. Therefore the typical continuous time models with isolated and independent jumps may not provide a good description of stochastic commodity prices. The Markov regime switching (RS) model first proposed by Hamilton (1989) is a promising model for commodity prices. In a RS model, spot prices can jump discontinuously between different states governed by state probabilities and model parameters. The RS model can be used to capture the shifts between "abnormal" and "normal" equilibrium states of supply and demand for a commodity.

Versions of the RS model have previously been applied to the investigation of business cycle asymmetry in Hamilton (1989) and Lam (1990), heteroscedasticity in time series of asset prices in Schwert (1996), the effects of oil prices on U.S. GDP growth in Raymond and Rich (1997). RS specifications for modeling stochastic commodity prices are studied in Deng (2000) and de Jong (2005) for electricity prices and in Chen and Forsyth (2008) for natural gas prices. Deng (2000) shows that by incorporating jumps and regime switching in modeling electricity prices, as opposed to the commonly used GBM model, the values of short-maturity out-of-the-money options approximate market prices very well. de Jong (2005) indicates that RS models are better able to capture the market dynamics than a GARCH(1,1) or Poisson jump model. Chen and Forsyth (2008) show that the RS model outperforms traditional one-factor MR model by solving the gas storage pricing problem using numerical techniques.

In this paper, we examine the application of a RS model to lumber prices to investigate whether it represents an improvement over a single regime model that has been used previously in the forestry literature. We will use the prices of lumber derivatives to calibrate the parameters of the price process in each of two regimes, and compare with the results of assuming a single regime. Allowing for two regimes may be thought of as a generalization of the more restrictive one regime case. The two regimes may be seen as representing two distinct sets of parameter values, perhaps reflecting good and bad times, in which the volatility, long run equilibrium price level and speed of mean reversion are all able to change. It is hoped that the two regimes may be a rich enough description of timber prices so that the addition of other stochastic factors is unnecessary.

3 A first look at lumber markets and prices

Since our concern is with modelling timber prices and evaluating an optimal tree harvesting problem in Canada, a brief review the forest products industry is in order as well as the presentation of some descriptive statistics for Canadian spot lumber prices over the past decade.

Forest products, including logs, lumber, and paper, are traded worldwide and Canada is a major player in this market, accounting for 14% of the value of world forest product exports in 2006.[6] Forest products are a significant component of Canada's balance of trade, with forest product exports amounting to $29 billion (Canadian) in 2006, which was 5.4% of total exports of goods and services. Note that this is down from a peak of $43 billion in 2000. Canada's forest product exports are mainly destined for the United States (over 75% went to the U.S. in 2006) and Canada is the source of over 80% of U.S. lumber imports.[7] More than half of Canadian lumber exports come from British Columbia, followed with Quebec and Ontario.

Forest product prices in North America are affected by swings in housing starts and other demand sources, supply factors such as fire and pests that plague forests from time to time, regulatory changes and by the increased integration of forest product markets worldwide. In addition, forest operations in Canada have been severely affected by on-going trade disputes between Canada and the U.S. Forest product prices are almost all quoted in U.S. dollars, which is an added source of volatility for Canadian forest product producers who receive revenue in U.S. dollars but pay silviculture and harvesting costs in Canadian dollars. Participants in forest product markets can hedge some risks by buying or selling futures contracts. Lumber futures contracts with expiry dates for up to one year in the future have been traded on the Chicago Mercantile Exchange (CME) since 1969.

Real weekly spot prices for Canadian lumber are shown in Figure 1. Periods of boom and bust are evident in the diagram, with the especially difficult time in the industry clearly apparent from mid-2004 onward. This reflects declining lumber prices in the United States as well as the appreciation of the Canadian dollar which rose from from 0.772 $U.S./$Cdn in January 2004 to 0.998 $U.S./$Cdn in January 2008. Descriptive statistics for the lumber price time series and its corresponding return are provided in Table 1. Return is calculated as $ln(P_t/P_{t-1})$ where P_t refers to price at time t. Weekly data is used, however, the minimum, maximum, and mean returns as well as the standard deviation have been annualized. The returns of the price time series exhibit excess kurtosis, which implies that a pure GBM model is not able to fully describe the dynamics of lumber price process.[8] A QQ-plot and a

[6]Source: FAOstat database, Food and Agricultural Organization of the United Nations, *http://faostat.fao.org/site/381/DesktopDefault.aspx?PageID=381*

[7]Source: Canada's Forests, Statistical Data, Natural Resources Canada, *http://canadaforests.nrcan.gc.ca/statsprofileCanada* (retrieved May 4, 2008), and Random Lengths, "Yardstick"

[8]A GBM model implies that price follows a log normal distribution. For a normal distribution skewness is zero and kurtosis is three.

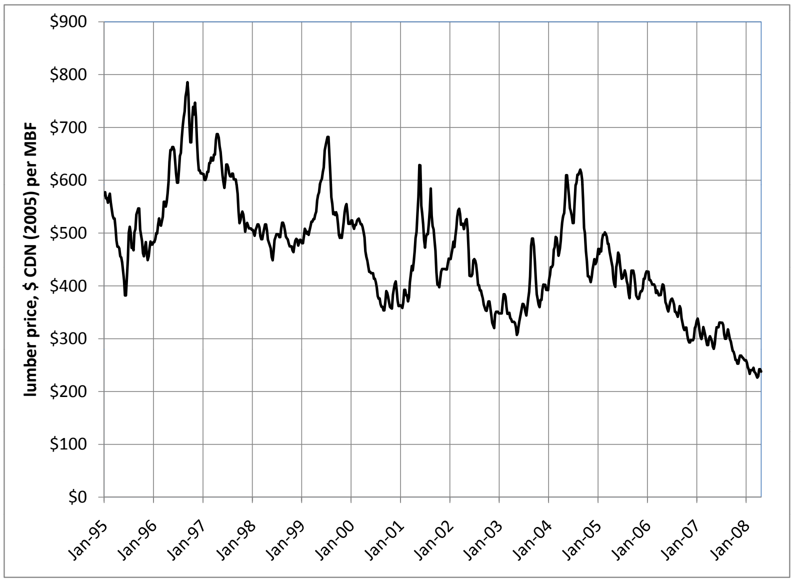

FIGURE 1: *Real prices of softwood lumber, Toronto, Ontario. Weekly data from January 6th, 1995 to April 25th, 2008, \$Cdn./MBF, (MBF ≡ thousand board feet) Nominal prices deflated by the Canadian Consumer Price Index, base year = 2005.*

Item	Max	Min	Mean	Std. Dev.	Skewness	Kurtosis
Cdn (2005) $/MBF	785.6	226.5	459.3	109.6	0.2151	2.711
Return	653.0 %	-644.5 %	-6.5 %	21.5 %	0.134	4.448

TABLE 1: *Descriptive statistics for the lumber price time series (as shown in Figure 1) and its returns, from January 6th, 1995 to April 25th, 2008. The return is the continuously compounded return calculated on weekly data. Minimum, maximum, mean and standard deviation of return are annualized.*

histogram are presented in Figure 2. Fat tails shown in the QQ-plot also indicate that the return series does not follow a normal distribution. A formal test of normality (the Jarque-Bera test) strongly rejects the null hypothesis that return follows a normal distribution.

4 Calibration of Lumber Spot Price Models

In this section we specify and parameterize the two timber price models that will be used in our optimal harvesting problem. The models we consider are a traditional mean reverting process (TMR) as used in Insley and Rollins (2005) and Insley and Lei (2007) and a regime switching model in which the spot price follows potentially two different mean reverting processes (the RSMR model). We calibrate the two models using lumber derivatives prices and present evidence as to which can better describe timber prices.

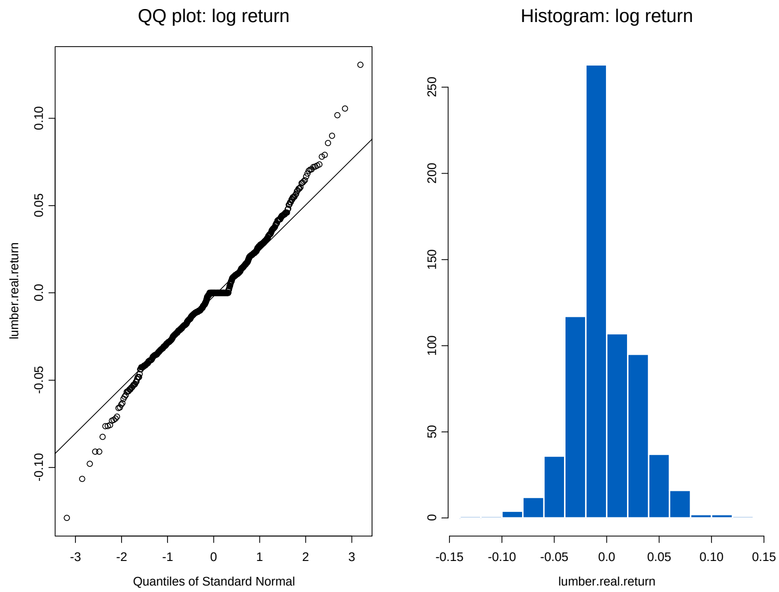

FIGURE 2: *QQ-plot and histogram of return process.*

The RSMR model for lumber price, P, is given by the following stochastic differential equation (SDE):

$$dP = \alpha(s_t)(K(s_t) - P)dt + \sigma(s_t)PdZ \tag{4}$$

where s_t is a two-state continuous time Markov chain, taking two values 0 or 1. The value of s_t indicates the regime in which the lumber price resides at time t. Define a Poisson process $q^{s_t \to 1-s_t}$ with intensity $\lambda^{s_t \to 1-s_t}$. Then

$$\begin{aligned} dq^{s_t \to 1-s_t} &= 1 \qquad \text{with probability } \lambda^{s_t \to 1-s_t}dt \\ &= 0 \quad \text{with probability } 1 - \lambda^{s_t \to 1-s_t}dt \end{aligned}$$

In other words, the probability of regime shifts from s_t to $(1 - s_t)$ during the small time interval dt is $\lambda^{s_t \to 1-s_t}dt$. The probability of the lumber price staying in the current regime s_t is $1 - \lambda^{s_t \to 1-s_t}dt$.

In this RSMR model, each parameter in the equation is allowed to shift between two states implied by s_t. $K(s_t)$ is the long-run equilibrium level to which the price tends toward following any disturbance. We refer to $\alpha(s_t)$ as the mean reversion rate; the higher its value the more quickly price reverts to its long run mean value. $\sigma(s_t)$ denotes price volatility; dZ is the increment of the standard Wiener process. The stochastic factors for the two regimes are perfectly correlated. Therefore there is a common dZ for two different SDE.

The TMR model, which is calibrated for comparison with the RSMR model, is described by the following stochastic differential equation:

$$dP = \alpha(K - P)dt + \sigma PdZ \tag{5}$$

where dZ is an increment of the standard Wiener process. In contrast with RSMR model, the parameters in the above equation are constant, instead of being regime dependent, Ideally we would rely on statistical tests to determine which of Equation (4) or Equation (5) is a better model of lumber prices. However, since the parameter $\lambda^{s_t \to 1-s_t}dt$ is defined only in relation to s_t in Equation (4) and is not present in (5), the traditional asymptotic tests such as the likelihood ratio, Lagrange multiplier and Wald tests do not have a standard asymptotic distribution and cannot be used (Davies (1977), Davies (1987)). As is detailed later in this section, we rely on the calibration procedure to determine whether the regime switching model is able to adequately describe lumber prices.

We require estimates of the parameters of our two proposed lumber price models, Equations (4) and (5). Traditionally parameter estimation is done using time series data on spot prices. However parameter estimates obtained in this manner reflect the actual probability distribution of the stochastic variable - the so-called P-measure. In valuing investments contingent on a stochastic process estimated in the P-measure, it is necessary to consider risk aversion by estimating a market price of risk.

For the regime switching model, Hamilton (1989) presents a nonlinear filter and smoother to get statistical estimates of the unobserved state, s_t, given observations on values of P_t. The marginal likelihood function of the observed variable is a byproduct of the recursive filter, allowing parameter estimation by maximizing this likelihood function. The parameters estimated in this way are under the P-measure implying that a corresponding market price of risk has to be estimated as well.

In contrast to Hamilton's method, in Chen and Forsyth (2008) the parameters of the risk-adjusted processes are calibrated by using natural gas derivative contracts, meaning that the parameters thus estimated are under the risk neutral probability measure, Q-measure, allowing the assumption of risk neutrality in the subsequent contingent investment valuation. In this paper, we follow a similar procedure to Chen and Forsyth (2008) using lumber derivatives, and present the details here for the convenience of the reader. For all parameter values except the volatilities, lumber futures contracts are used in the calibration process. For reasons explained below, options on lumber futures are used to calibrate volatilities.

4.1 Calibration using futures prices

Ito's lemma is used to derive two partial differential equations characterizing lumber futures prices. These partial differential equations are simplified to a system of ordinary differential equations which can be solved numerically to give futures prices consistent with different parameter values. The calibration procedure determines those parameter values (except for the volatilities) which produce calculated futures prices that most closely match a time series of market futures prices.

Beginning with the TMR model, let $F(P, t, T)$ denote the futures price at time t with maturity T. A futures contract is a contingent claim. From Ito's lemma, the PDE describing the futures price is given by Equation (6).

$$F_t + \alpha(K - P)F_P + \frac{1}{2}\sigma^2 P^2 F_{PP} = 0. \tag{6}$$

At the expiry date T the futures price will equal the spot price, which gives the boundary condition: $F(P, T, T) = P$

The solution of this PDE is known to have the form

$$F(P,t,T) = a(t,T) + b(t,T)P. \tag{7}$$

Substituting Equation (7) into Equation (6), gives the following ODE system

$$\begin{aligned} a_t + \alpha K b &= 0 \\ b_t - \alpha b &= 0 \end{aligned} \tag{8}$$

where $a_t \equiv \partial a/\partial t$ and $b_t \equiv \partial b/\partial t$. The boundary conditions: $a(T,T) = 0$; $b(T,T) = 1$ are required in order for $F(P,T,T) = P$ to hold.

Next for the RSMR model, let $F(s_t, P, t, T)$ denote lumber futures price at time t with maturity T in regime s_t, where $s_t \in \{0, 1\}$. The no-arbitrage value $F(s_t, P, t, T)$ can be expressed as the risk neutral expectation of the spot price at T.

$$F(s_t, P, t, T) = E^Q[P(T)|P(t) = p, s_t]. \tag{9}$$

The lumber futures price is a derivative contract whose value depends on the stochastic price and the corresponding regime. Using Ito's lemma for a jump process the conditional expectation satisfies two PDEs, one for each regime, given by:

$$F(s_t)_t + \alpha(s_t)(K(s_t) - P)F(s_t)_P + \frac{1}{2}\sigma(s_t)^2 P^2 F(s_t)_{PP} + \lambda^{s_t \to (1-s_t)}(F(1-s_t) - F(s_t)) = 0 \tag{10}$$

with the boundary condition: $F(s_t, P, T, T) = P$.

The solution to these PDEs is known to have the form

$$F(s_t, P, t, T) = a(s_t, t, T) + b(s_t, t, T)P. \tag{11}$$

This yields the following ordinary differential equation (ODE) system,

$$\begin{aligned} a(s_t)_t + \lambda^{s_t \to (1-s_t)}(a(1-s_t) - a(s_t)) + \alpha(s_t)K(s_t)b(s_t) &= 0 \\ b(s_t)_t - (\alpha(s_t) + \lambda^{s_t \to (1-s_t)})b(s_t) + \lambda^{s_t \to (1-s_t)}b(1-s_t) &= 0 \end{aligned} \tag{12}$$

with boundary conditions $a(s_t, T, T) = 0$; $b(s_t, T, T) = 1$. $a(s_t)_t \equiv \partial a(s_t)/\partial t$ and $b(s_t)_t \equiv \partial b(s_t)/\partial t$. These ODEs will be solved numerically, which gives the model parameters. This is detailed in Section 5.

Note that the volatility σ does not appear in Equations (8) and (12). Hence we cannot use lumber futures prices to calibrate the spot price volatility. As in Chen and Forsyth (2008), lumber futures option prices are used to calibrate the volatility.

A least squares approach is used for calibrating the risk-neutral parameter values. Let θ denote the set of parameters calibrated to the futures price data, where $\theta_{RSMR} = \{\alpha(s_t), K(s_t), \lambda^{s_t \to (1-s_t)} | s_t \in \{0, 1\}\}$ and $\theta_{TMR} = \{\alpha, K\}$. In particular, at each observation day t, where $t \in \{1, ..., t^*\}$, there are T^* futures contracts with T^* different maturity dates. For the RSMR model the calibration is performed by solving the following optimization problems:

$$\min_\theta \sum_t \sum_T (\hat{F}(\hat{s}_t(\theta), P(t), t, T; \theta) - F(t,T))^2 \tag{13}$$

where $F(t,T)$ is the market futures price on the observation day t with maturity T. $\hat{F}(\hat{s}_t(\theta), P(t), t, T; \theta)$ is the corresponding model implied futures price computed numerically determined in equation (11) using the market spot price $P(t)$ and the parameter set θ in regime $\hat{s}_t(\theta)$, where

$$\hat{s}_t(\theta) = \underset{s_t \in \{0,1\}}{\operatorname{argmin}} \sum_T (\hat{F}(s_t, P(t), t, T; \theta) - F(t,T))^2 \tag{14}$$

At each t, the regime $\hat{s}_t(\theta)$ will be determined by minimizing the sum of squared errors between the market futures prices F, and the corresponding model implied futures prices $\hat{F}$, for all T^* at t for a given θ. The calibrated parameter set θ will then minimize the distance between F and $\hat{F}$ for all t^*.

Similarly, for TMR model, the optimization problem becomes

$$\min_\theta \sum_t \sum_T (\hat{F}(P(t), t, T; \theta) - F(t,T))^2 \tag{15}$$

where $\hat{F}(P(t), t, T; \theta)$ is the model implied futures price.

4.2 Calibration of volatilities using options on futures

In this section, the spot price volatility is calibrated for the two different price models using market European call options on lumber futures. For the RSMR model, let $\bar{V}(s_t, F, t, T_v)$ denote the European call option value on the underlying lumber futures contract F at time t with maturity at T_v in regime s_t. $F(s_t, t, T)$ represents the value of the underlying futures contract at time t with maturity at T, where $T \geq T_v$. Let X be the strike price of option. In the risk-neutral world, $\bar{V}(s_t, F, t, T_v)$ can be expressed as

$$\bar{V}(s_t, F, t, T_v) = e^{-r(T_v - t)} E^Q[\max(F(s_T, T_v, T) - X, 0) | F(s_t, t, T) = F, s_t] \tag{16}$$

If the lumber options expiration date T_v is the same as that of the underlying futures T, $\bar{V}(s_t, F, t, T_v) = \bar{V}(s_t, F, t, T)$ and $F(s_T, T_v, T) = F(s_T, T, T)$. Therefore the above equation can be transformed to

$$\begin{aligned} \bar{V}(s_t, F, t, T) &= e^{-r(T-t)} E^Q[\max(F(s_T, T, T) - X, 0) | F(s_t, t, T) = F, s_t] \\ &= e^{-r(T-t)} E^Q[\max(P(T) - X, 0) | a(s_t, t, T) + b(s_t, t, T) P(t) = F, s_t] \end{aligned} \tag{17}$$

where $P(T)$ is the lumber spot price and $F(s_T, T, T) = P(T)$ at the maturity date T.

For calibration purposes, a hypothetical European call option is needed. Let $V(s_t, P, t, T)$ denote such a call option on lumber at time t with maturity T in regime s_t. This option value can be expressed in the form of the risk-neutral expectation as

$$V(s_t, P, t, T) = e^{-r(T-t)} E^Q[\max(P(T) - X, 0) | P(t) = P, s_t] \tag{18}$$

Given that lumber price P follows RSMR, the option value $V(s_t, P, t, T)$ satisfies the coupled PDEs

$$\begin{aligned} V(s_t)_t + \alpha(s_t)(K(s_t) - P) V(s_t)_P + \frac{1}{2}\sigma(s_t)^2 P^2 V(s_t)_{PP} - rV(s_t) + \\ \lambda^{s_t \to 1 - s_t}[V(1 - s_t) - V(s_t)] = 0 \end{aligned} \tag{19}$$

with the boundary condition: $V(s_t, P, T, T) = \max[P(T) - X, 0]$. The value of this hypothetical option $V(s_t, P, t, T)$ can be solved numerically by solving the above PDEs.

Comparing equations (17) and (18), the following relationship holds.

$$\bar{V}(s_t, F, t, T) = V(s_t, \frac{F - a(s_t, t, T)}{b(s_t, t, T)}, t, T) \tag{20}$$

where $a(s_t, t, T)$ and $b(s_t, t, T)$ can be calculated based on Equation (12). Therefore, after getting $V(s_t, P, t, T)$ by solving the equation (19), the theoretical lumber option value $\bar{V}(s_t, F, t, T)$ can be calculated using the interpolation method.

Similarly, for the TMR model, let $\bar{V}(F, t, T)$ and $V(P, t, T)$ represent the European call option on lumber futures and the hypothetical European call option on lumber respectively.[9] The corresponding PDE for characterizing $V(P, t, T)$ is expressed as

$$V_t + \alpha(K - P)V_P + \frac{1}{2}\sigma^2 P^2 V_{PP} - rV = 0 \tag{21}$$

with boundary condition: $V(P, T, T) = \max[P(T) - X, 0]$. Given the relationship[10]

$$\bar{V}(F, t, T) = V(\frac{F - a(t, T)}{b(t, T)}, t, T) \tag{22}$$

the model implied option value $\bar{V}(F, t, T)$ can be computed after getting $V(P, t, T)$ by solving the above PDE.

A least squares approach is also used to calibrate the volatility. In particular for the RSMR model, after determining the optimal regime $\hat{s}_t$ based on the approach described in the previous section, we solve the following optimization problem:

$$\min_{\sigma(0),\sigma(1)} \sum_X (\bar{V}(\hat{s}_t, F(t, T), t, T; \theta, X, \sigma(0), \sigma(1)) - V(t, T; X))^2 \tag{23}$$

where $\bar{V}(\hat{s}_t, F, t, T; \theta, X, \sigma(0), \sigma(1))$ represents the corresponding model implied option value at time t with maturity T, strike price X and the parameter values θ calibrated in the previous section and $V(t, T; X)$ is the market value of lumber call option on futures. T^* option contracts with T^* different strike prices are needed for volatility calibration. The calibrated parameter set $\{\sigma(0), \sigma(1)\}$ will minimize the square distance between $\bar{V}$ and V.

Similarly, for the TMR model, the optimization problem becomes:

$$\min_{\sigma} \sum_X (\bar{V}(F(t, T), t, T; \theta, X, \sigma) - V(t, T; X))^2 \tag{24}$$

5 Calibration results and testing of the models

5.1 Data description: Lumber futures and options on futures

Lumber market futures and options on futures are used to calculate the risk neutral spot price process. Four different futures contracts corresponding to each observation date for every

[9] $T_v \approx T$ in this model as well.

[10] This relationship is derived in the same way as equation (20).

Friday from January 6th, 1995 to April 25th, 2008 will be employed in the calibration. The average maturity days for these four futures contracts which trade on the Chicago Mercantile Exchange (CME), are about 30, 90, 150 and 210. Since we are interested in estimating the stochastic process for real lumber prices for a Canadian forestry problem, future prices were deflated by the consumer price index and converted to Canadian dollars.[11]

The future call options used to calibrate volatilities are also from the CME. Two sets of six call options written on the same futures contract were chosen. The call options expire on October 31st, 2008 while the underlying futures contract expires on November 14, 2008. (At the CME, the lumber options expire the last business day in the month prior to the delivery month of the underlying futures contract.) The first set of six options was obtained on May 23rd, 2008 and the price of the corresponding futures contract was 260.8 $U.S./mbf. The second set was obtained on May 30th, 2008 and the futures price on that day was 260.9 $U.S./mbf. The strike prices of the six call options range from 260 to 310 $U.S./mbf.

In our case since the underlying futures contracts expires on November 14, 2008 and the options expire on October 31, 2008, $T_v < T$. For the calibration, we must assume that $T_v = T$ holds approximately. To justify this assumption, we appeal to the fact that options prices were retrieved in May 2008, some months before their expiry.

5.2 Calibration Results

Table 2 presents the calibration results for parameter values in the RSMR model.[12] In the table we observe two quite different regimes in the Q-measure. Regime 1 has a much higher equilibrium price level, $K(1)$, but a lower speed of mean reversion, $\alpha(1)$ compared to regime 0. The risk neutral intensity of switching out of regime 1 is very low at $\lambda^{1\to 0} = 0.39$ which implies that in the risk neutral world prices are mostly in this regime with the higher equilibrium price.

Calibrated parameter values for the TMR model are also reported in Table 2. Compared with the RSMR model, for the TMR model, both the long-run price level K and mean reversion rate α are between the values reported for regime 1 and regime 0.

Table 3 reports the mean absolute errors as defined in Equations (13) and (14) for the four futures contracts used to calibrate the RSMR and the TMR models. From the last column, it appears that the RSMR model outperforms the TMR model, since the overall average errors expressed in two different ways are lower in the RSMR model. The RSMR model also has lower errors for each of the four futures contracts individually. Figures 3 and 4 show plots of the the model implied futures prices and market futures prices for the two futures contracts corresponding to the largest and smallest calibration errors from Table 3.

[11] For CME Random Length Lumber futures, the delivery contract months are as follows: January, March, May, July, September and November. There are six lumber futures on each day only the first four of which are actively traded. Therefore, only the first four futures contracts are used in parameter calibration. The last day of trading is the business day prior to the 16th calendar day of the contract month.

[12] Since these parameters are calibrated in the Q-measure it is not possible to interpret them in terms of the observed behaviour of spot prices. However, if the market price of risk equals zero the P-measure and Q-measure will coincide. If we believe that the market price of risk for a commodity is fairly low then we can draw some intuition about the P-measure process from our results.

RSMR Model

$\alpha(0)$	$\alpha(1)$	$K(0)$	$K(1)$	$\lambda^{0\to1}$	$\lambda^{1\to0}$
3.61	0.40	71.92	516.64	17.09	0.39

TMR Model

α	K
0.69	341.00

TABLE 2: *Calibrated parameter values for the RSMR and TMR model, $K(0)$, $K(1)$ and K are in \$Cdn(2005)/MBF.*

Mean absolute error					
T	30	90	150	210	Overall
RSMR model					
In dollars	22.23	18.50	18.97	20.56	20.07
In percentage	5.65	4.49	4.56	5.00	4.93
TMR model					
In dollars	39.33	30.90	30.49	34.48	33.80
In percentage	10.36	7.85	7.48	8.21	8.47

TABLE 3: *Mean absolute errors for all the four different futures contracts in both RSMR and TMR models, expressed in dollars and in percentage. T refers to the number of days to maturity*

The closer fit of the RSMR model to market data is noticeable through visual inspection of these graphs.

We perform a χ^2 test to determine more rigourously if our calibration procedure produces a good fit of the futures data. A time series of the difference between the model implied futures prices and market futures prices can be calculated for each model and the mean of this series is tested to determine whether it is statistically different from zero. Let $\hat{F}$ denotes model implied futures prices and F refers to the market futures prices. The difference of these two time series can be expressed as

$$\text{diff}_t = \hat{F}_t - F_t \tag{25}$$

for all the observation dates $t \in T$. Define μ_{diff} as the mean of the difference and σ^2_{diff} as the variance of the difference. Therefore $\hat{\mu}_{\text{diff}}$ and $\hat{\sigma}^2_{\text{diff}}$ refer to the estimator of the mean and variance respectively. The null of the test is $H_0 : \mu_{\text{diff}} = 0$. The alternative is $H_1 : \mu_{\text{diff}} \neq 0$. The test statistic for the mean of this difference can be constructed as

$$\frac{\hat{\mu}^2_{\text{diff}}}{\hat{\sigma}^2_{\text{diff}}} \sim \chi^2_{(1)} \tag{26}$$

Test statistics and corresponding P-values are calculated for all four futures contracts for both models. The results are shown in Table 4.

From Table 4 for both the RSMR and TMR models, we cannot reject the null at the 1% level for all four futures contracts. So for both models the difference between the model

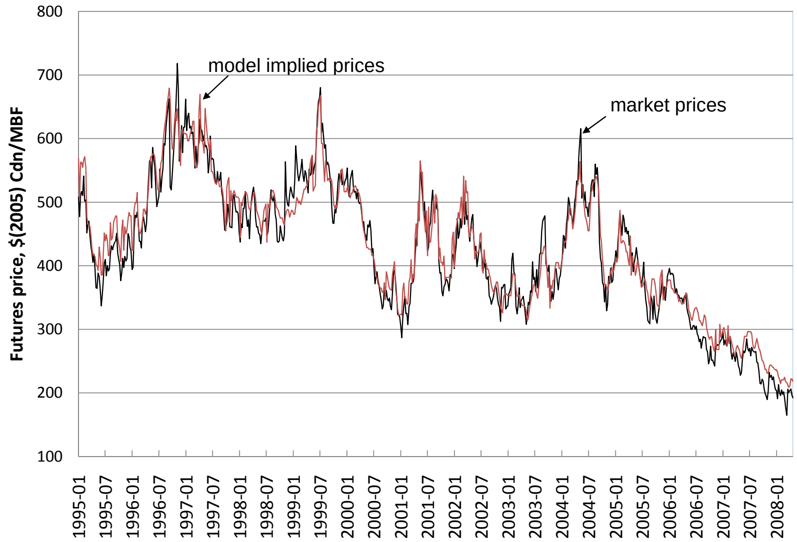

(A) *f1: futures contracts with average 30 days to maturity.*

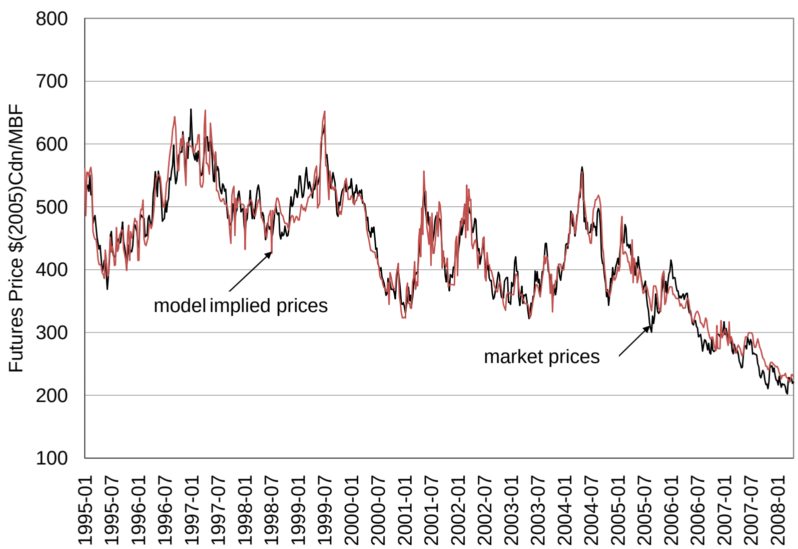

(B) *f2: futures contract with average 60 days to maturity.*

FIGURE 3: *RSMR model implied futures prices and market futures prices for two futures contracts. f1 has the largest error while f2 has the smallest error in Table 3.*

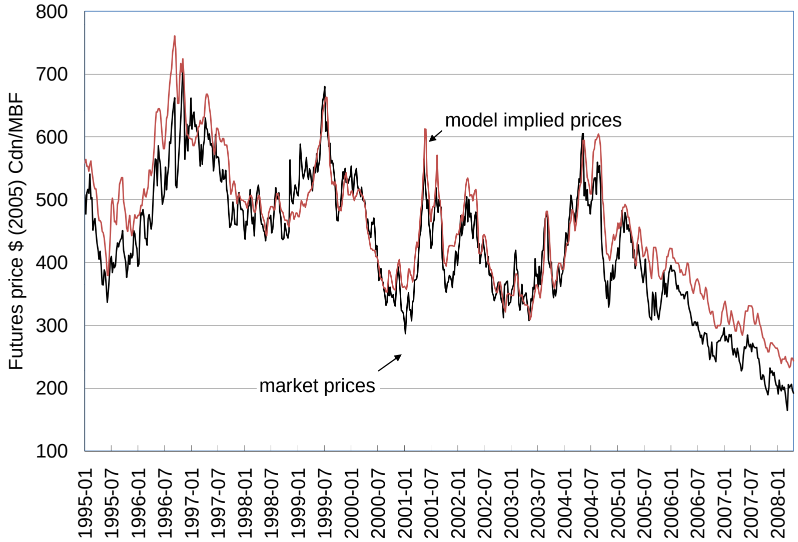

(A) *f1: futures contracts with average 30 days to maturity.*

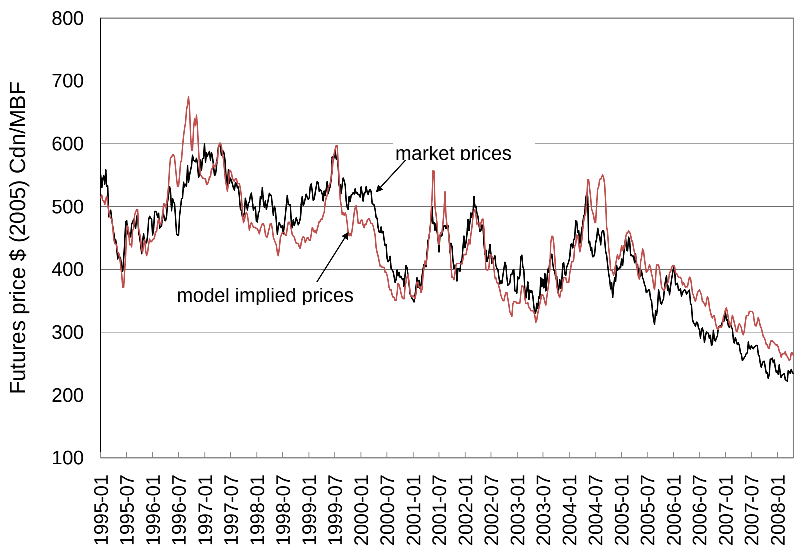

(B) *f3: futures contracts with average 90 days to maturity.*

FIGURE 4: *TMR model implied futures prices and market futures prices for two futures contracts, f1 has the largest error while f3 has the smallest error from Table 3.*

Model diagnostic check				
T	30	90	150	210
RSMR model				
Test statistics	0.0947	0.0000	0.0005	0.0010
p-value	0.7583	0.9964	0.9820	0.9750
TMR model				
Test statistics	0.5918	0.1251	0.0000	0.0863
p-value	0.4417	0.7236	0.9976	0.7689

Table 4: *Model diagnostic check for RSMR and TMR models*

RSMR Model		TMR Model
$\sigma(0)$	$\sigma(1)$	σ
0.0038	0.2545	0.28

Table 5: *Calibrated volatilities for the RSMR and TMR models*

implied and actual futures prices is not significant for all contracts. By this measure our calibration procedure has done a good job at matching futures prices to both the TMR and RSMR models. Unfortunately this test does not allow us to conclude that one model is definitely preferred over the other. In the next section we will consider whether the choice of TMR or RSMR model makes a difference to the optimal decision in a timber harvesting problem.

The calibration procedure on futures options, described in Section 4.2, resulted in calibrated volatilities shown in Table 5. Volatility in regime 0 is much lower than in regime 1. It may be noted that $\lambda^{0\to1}$ is quite high, indicating that in the risk neutral world price remains only briefly in regime 0. The expected time in a given regime is $1/\lambda$ years.

6 Specification of the optimal harvesting problem and its numerical solution

After analyzing the dynamics of the lumber price process and calibrating all the parameter values of the corresponding model, we are ready to solve for the value a forestry investment. We will value a hypothetical stand of trees in Ontario's boreal forest using both the RSMR and TMR models. We will investigate whether use of these two models in a realistic optimal harvesting problem will result in different land values and optimal harvesting ages. We use the same investment problem as in Insley and Lei (2007). In Insley and Lei (2007) a TMR process was used and the estimation procedure was carried out through ordinary least squares on spot price data. We compare the regime switching model with the results of the TMR process and also the results from Insley and Lei (2007).

In the following sections, a real options model of the forestry investment valuation will be developed assuming lumber prices follow the RSMR process. Coupled partial differential equations (PDEs) characterizing the values of the option to harvest the trees will be derived using contingent claim analysis. A finite difference method will be employed to solve the PDEs numerically given appropriate boundary conditions. The model and numerical solution scheme for the TMR price case is described in Insley and Rollins (2005).

6.1 Harvesting model for the RSMR case

We model the optimal decision of the owner of stand of trees who wants to maximize the value of the stand (or land value) by optimally choosing the harvest time. It is assumed that forestry is the best use for this land, so that once the stand is harvested it will be allowed to grow again for future harvesting. Since this is a multirotational optimal harvesting problem, it represents a path-dependent option. The value of the option to harvest the stand today depends on the quantity of lumber, which itself depends on the last time when the stand was harvested.

Lumber price is assumed to follow either the RSMR model or the TMR model detailed in the previous sections. In this section we derive the key partial differential equation that describes the value of the stand of trees for the RSMR case. Derivation of the key partial differential equation for the TMR case can be found in Insley and Lei (2007).

For now we write the RSMR model from Equation (4) in a more general form as:

$$dP(s_t) = a(s_t, P, t)dt + b(s_t, P, t)dZ \tag{27}$$

Denote $q^{s_t \to 1-s_t}$, the risk of regime shift, as a Poisson process, where $s_t \in \{0, 1\}$ indicates the regime.

$$\begin{aligned} dq^{s_t \to 1-s_t} &= 1 \quad \text{with probability } \lambda^{s_t \to 1-s_t} dt \\ dq^{s_t \to 1-s_t} &= 0 \quad \text{with probability } 1 - \lambda^{s_t \to 1-s_t} dt \end{aligned}$$

With probability λdt price changes regime during the small interval dt, and with probability $1 - \lambda dt$ price remains in the same regime.

There are two risks associated with this stochastic process. One is the standard continuous risk in the dZ term. The other, in discrete form, is due to the risk of regime switch. In order to hedge these two risks and value the stand of trees $V(s_t, P, \varphi)$, two other traded investment assets, which depend solely on lumber price, are needed. Let φ denote the age of the stand, defined as $\varphi = t - t_h$, where t_h represents the time of last harvest. φ in this case is another state variable, in addition to P. φ satisfies $d\varphi = dt$.

Assume that there exist investment assets which depend on the lumber price P and can be used to hedge the risk of our investment. Using standard arguments we set up a hedging portfolio that eliminates the two risks. We can derive the fundamental partial differential equation that characterizes the value of the stand of trees.

$$\begin{aligned} V(s_t)_t + (a(s_t, P, t) - \beta_P b(s_t, P, t))V(s_t)_P + \frac{1}{2} b(s_t, P, t)^2 V(s_t)_{PP} + \\ V(s_t)_\varphi - rV(s_t) + \beta_{sw}(V(1 - s_t) - V(s_t)) = 0 \end{aligned} \tag{28}$$

β_P and β_{sw} are parameters which represent market prices of risk for the diffusion risk and regime-switching risk respectively.

Our estimation method detailed in Sections 4 and 5 yields risk neutral parameter values. Therefore the following relationships hold

$$\begin{aligned}
a(s_t, P, t) - \beta_P b(s_t, P, t) &= \alpha(s_t)(K(s_t) - P) \\
b(s_t, P, t) &= \sigma(s_t)P \\
\beta_{sw} &= \lambda^{s_t \to 1-s_t}
\end{aligned}$$

Substituting these equations into the above PDE give

$$V(s_t)_t + \alpha(s_t)(K(s_t) - P)V(s_t)_P + \frac{1}{2}(\sigma(s_t)P)^2 V(s_t)_{PP} + V(s_t)_\varphi - rV(s_t) + \lambda^{s_t \to 1-s_t}(V(1 - s_t) - V(s_t)) = 0. \tag{29}$$

The complete harvesting problem can then be specified as a linear complementarity problem (LCP). Define $\tau \equiv T - t$ as time remaining in the option's life. Rewrite the above PDE and define HV as

$$HV \equiv rV(s_t) - (V(s_t)_t + \alpha(s_t)(K(s_t) - P)V(s_t)_P + \frac{1}{2}(\sigma(s_t)P)^2 V(s_t)_{PP} + V(s_t)_\varphi + \lambda^{s_t \to 1-s_t}(V(1 - s_t) - V(s_t))) \tag{30}$$

Then the LCP is modeled as:

$$\begin{aligned}
&(i) \quad HV \geq 0 \\
&(ii) \quad V(s_t, P, \varphi) - [(P - C_h)Q(\varphi) + V(s_t, P, 0)] \geq 0 \\
&(iii) \quad HV\Big[V(s_t, P, \varphi) - [(P - C_h)Q(\varphi) + V(s_t, P, 0)]\Big] = 0
\end{aligned} \tag{31}$$

where C_h is the cost per unit of lumber, $Q(\varphi)$ is the volume of the lumber which is a function of age, $Q = g(\varphi)$. $[(P - C_h)Q(\varphi) + V(s_t, P, 0)]$ is the payoff from harvesting immediately and consists of revenue from selling the harvested timber plus the value of the bare land, $V(s_t, P, 0)$. The above LCP implies if the stand of trees is managed optimally either HV, $V(s_t, P, \varphi) - [(P - C_h)Q(\varphi) + V(s_t, P, 0)]$, or both will be equal to zero. If $HV = 0$, it is optimal for the investor to continue holding the option by delaying the decision to harvest. The growing stand of trees is earning the risk free return. If $V(s_t, P, \varphi) - [(P - C_h)Q(\varphi) + V(s_t, P, 0)] = 0$, then the value of the stand of trees just equals the value of immediate harvest and the investor should harvest the trees. If both terms are equal to zero, either strategy is optimal.

6.2 Numerical solution of the Linear Complementarity Problem

This section briefly describes the numerical methods used for solving the regime switching LCP, Equation (31). We also analyze the properties of the scheme, such as the stability and monotonicity. More details of the numerical solution are contained in Appendix A.

6.2.1 General description of the numerical methods

The option to choose the optimal harvest time has no analytical solution. The LCP expressed in Equation (31) in this paper is solved numerically using the combination of fully implicit finite difference method, semi-Lagrangian method and the penalty method. This approach is also used in Insley and Lei (2007) but for a single regime problem. The finite difference method is used to convert a differential equation into a set of discrete algebraic equations by replacing the differential operators in PDEs with finite difference operators.

For the optimal tree harvesting problem examined in this paper, there are two state variables. One is the spot price P and the other is the stand age φ. Using the semi-Lagrangian method this two-factor problem can be reduced to a one factor problem for each time step. After each time step, the true option value is obtained by using linear interpolation. For the details of this method, see Insley and Rollins (2005) and Morton and Mayers (1994).

There are several approaches to the numerical solution of the LCP. An overview of these methodologies is provided in Ikonen and Toivanen (2008). The penalty approach used here converts the LCP into a nonlinear algebraic problem, which is then solved by Newton iteration. The penalty method has several benefits. It is more accurate than an explicit method and has good convergence properties. Another advantage is that at each iteration it generates a well-behaved sparse matrix, which can be solved using either direct or iterative methods.[13]

The penalty method used in this paper is outlined here. Define $\tau = T - t$ and $V(s_t)_t = -V(s_t)_\tau$. The LCP[14] in Equation (31) can be expressed as a single equation:

$$V(s_t)_\tau - V(s_t)_\varphi = \alpha(s_t)(K(s_t) - P)V(s_t)_P + \frac{1}{2}(\sigma(s_t)P)^2 V(s_t)_{PP} - rV(s_t) + \lambda^{s_t \to 1-s_t}(V(1-s_t) - V(s_t)) + \Upsilon(s_t) \qquad (32)$$

where $\Upsilon(s_t)$ on the right hand side of this equation is the penalty term, which satisfies

$$\Upsilon(s_t) > 0 \text{ if } V(s_t, P, \varphi) = [(P - C_h)Q(\varphi) + V(s_t, P, 0)] \qquad (33)$$

$$= 0 \text{ if } V(s_t, P, \varphi) > [(P - C_h)Q(\varphi) + V(s_t, P, 0)] \qquad (34)$$

Equation (33) implies that if option value equals to the payoff, which is $[(P - C_h)Q(\varphi) + V(s_t, P, 0)]$[15], it is optimal to harvest the trees immediately, which is the first condition in LCP Equation (31). If the option value is higher than the payoff, Equation (34) implies the harvest should be delayed which is the second condition in the LCP equation. The penalty method in this way incorporates the American constraint.

A complicating factor in our problem is the presence of regime switching in the spot price process. We have two PDEs in the form of Equation (29), one for each option value of the two regimes. Moreover, the option value in one regime affects the option value in the other regime[16]. We deal with this problem by stacking the discretized version of equation (32) for

[13]See Zvan et al. (1998) and Fan et al. (1996) for more on the penalty method.

[14]This LCP characterizes the option value in regime s_t, $V(s_t)$.

[15]The payoff is defined as the net revenue of selling the trees plus the value of the bare land.

[16]i.e. The option value in regime $(1 - s_t)$, $V(1 - s_t)$, appears in Equation (29) characterizing the option value in regime s_t, $V(s_t)$.

option values in two regimes and solving the two discretized PDEs together at each time step. In this manner the PDEs in the two regimes are fully coupled.

6.2.2 Discretization

This section illustrates the main results of finite difference discretization, the semi-Lagrangian method and penalty method of dealing with LCP[17]. Prior to presenting the matrix form of the LCP discretization, several notations are introduced here.

For PDE discretization, unequally spaced grids in the directions of the two state variables P and φ are used. The grid points are represented by $[P_1, P_2, ..., P_{imax}]$ and $[\varphi_1, \varphi_2, ..., \varphi_{jmax}]$ respectively. We also discretize the time direction, represented as $\tau^N, ..., \tau^1$ ([18]). Define $V(s_t)_{ij}^{n+1}$ as an approximation of the exact solution $V(s_t, P_i, \varphi_j, \tau^{n+1})$, and $V^*(s_t)_{ij}^n$ as an approximation of $V(s_t, P_i, \varphi_j, \tau^n)$. Recall that $\tau = \tau^N$, $t = 0$ and at $\tau = \tau^1$, $t = T$. Based on the semi-Lagrangian method, the true solution of $V(s_t, P_i, \varphi_{j+\Delta\tau}, \tau^n)$ is obtained from $V^*(s_t)_{ij}^n$ using linear interpolation after each time step.

Denote ℓ a differential operator represented by

$$\ell V(s_t) = \alpha(s_t)(K(s_t) - P)V(s_t)_P + \frac{1}{2}(\sigma(s_t)P)^2 V(s_t)_{PP} - rV(s_t)$$

Equation (32) can be rearranged as:

$$V(s_t)_\tau - V(s_t)_\varphi = \ell V(s_t) + \lambda^{s_t \to 1-s_t} V(1-s_t) + \Upsilon(s_t) \tag{35}$$

Note that the right hand side of this equation has derivatives with respect to P only. Therefore this one-dimensional PDE for each φ_j is solved independently within each time step. After each time step is completed, using linear interpolation we will get $V(s_t, P_i, \varphi_{j+\Delta\tau}, \tau^n)$ from $V^*(s_t)_{ij}^n$. The discretized version of Equation (35) using the fully implicit method and the semi-Lagrangian method is written as

$$\frac{V(s_t)_{ij}^{n+1} - V^*(s_t)_{ij}^n}{\Delta\tau} = [\ell V(s_t)]_{ij}^{n+1} + \lambda^{s_t \to 1-s_t} V(1-s_t)_{ij}^{n+1} + \pi(s_t)_{ij}^{n+1} \tag{36}$$

where the penalty term $\pi(s_t)_{ij}^{n+1}$ is defined as

$$\pi(s_t)_{ij}^{n+1} = \frac{1}{\Delta\tau}(\text{payoff} - V(s_t)_{ij}^{n+1}) Large; \text{ if } V(s_t)_{ij}^{n+1} < \text{payoff} \tag{37}$$
$$= 0; \text{ otherwise} \tag{38}$$

The term 'Large' in equation (37) is a large number[19] and case dependent. The subscript ij refers to the point corresponding to (P_i, φ_j) and superscript n denotes the nth time step.

Rearranging Equation (36) and writing in a matrix form results in

$$W(s_t)V(s_t)^{n+1} - \Delta\tau\lambda^{s_t \to 1-s_t} V(1-s_t)^{n+1} = V^*(s_t)^n + \overline{\pi(s_t)}^{n+1} \text{payoff}(s_t)^{n+1} \tag{39}$$

[17]Detailed discretization is provided in Appendix A.

[18]The iteration starts from the final maturity date T and moves backward along the time direction until the current time 0.

[19]For example, $Large = 10^6$ for some cases.

where $W(s_t)$ is a sparse matrix containing all the parameters corresponding to the option value in regime s_t. The other terms except $\Delta\tau\lambda^{s_t \to 1-s_t}$ are expressed in vector form. The ijth element in the penalty vector $\overline{\pi(s_t)}^{n+1}$ is defined as

$$\begin{aligned}\overline{\pi(s_t)}_{ij}^{n+1} &= \mathit{Large};\ \text{if } V(s_t)_{ij}^{n+1} < \text{payoff} \\ &= 0;\ \text{otherwise}\end{aligned}$$

Equation (39) is the final discretized version of the LCP corresponding to $V(s_t)$. However, the option value in the other regime $V(1-s_t)$ appears in this expression. In order to obtain both option values for all the grid points at each time step, the discretized LCP for $V(1-s_t)$ which is similar with the expression (39) is stacked with Equation (39) to form a system of equations, which can be written as

$$Z_{matrix}\begin{bmatrix} V(s_t) \\ V(1-s_t) \end{bmatrix}^{n+1} = \begin{bmatrix} V^*(s_t) \\ V^*(1-s_t) \end{bmatrix}^{n} + \begin{bmatrix} \overline{\pi(s_t)} \\ \overline{\pi(1-s_t)} \end{bmatrix}^{n+1} \begin{bmatrix} \text{payoff}(s_t) \\ \text{payoff}(1-s_t) \end{bmatrix}^{n+1} \tag{40}$$

Z_{matrix} is a large sparse matrix. This system of equations is solved iteratively at each time step. For simplicity, the more compact version of Equation (40) can be expressed as

$$Z_{matrix}[V]^{n+1} = [V^*]^n + [\overline{\pi}]^{n+1}[\text{payoff}]^{n+1} \tag{41}$$

This is the scheme we use to numerically solve the optimal tree harvesting problem.

6.2.3 Boundary conditions and pseudo code

In order to solve Equation (41), the appropriate boundary conditions as well as the terminal condition are specified below. These are the same as used in Insley and Rollins (2005).

1. **As $\boldsymbol{P \to 0}$**, no specific boundary condition is needed. Substitute $P = 0$ into Equation (41) and discretize the resulted PDE.

2. **As $\boldsymbol{P \to \infty}$**, we set $V(s_t)_{PP} = 0$. As price goes to infinity, we assume the option value is a linear function of P.

3. **As $\boldsymbol{\varphi \to 0}$**, no specific boundary condition is needed since the PDE is first order hyperbolic in the φ direction, with outgoing characteristic in the negative φ direction.

4. **As $\boldsymbol{\varphi \to \infty}$**, $V(s_t)_\varphi \to 0$, and hence no boundary condition is needed. Since as the stand age goes to infinity, we assume the wood volume in the stand has reached some a steady state and the value of the option to harvest does not change with φ.

5. **Terminal condition.** $V(s_t, T) = 0$ This means when T gets very large, it has a negligible effect on the current option value.

Pseudo code for solving Equation (41) is provided as the follows[20].

[20] All programs are written in Matlab.

1. Set up tolerance level tol
2. $Large = \frac{1}{tol}$
3. for $\tau = 1 : N-1$; % time step iteration
for $j = 1 : jmax$; % iterate along the age φ direction
$([V]^{n+1})^0 = [V]^n$; % initial guess for $[V]^{n+1}$
for $k = 0, ...$ until convergence; % penalty American constraint iteration

$$\begin{aligned}(\overline{\pi}^{n+1})^k &= Large; \text{if } V^{n+1} < \text{payoff} \\ &= 0; \text{ otherwise}\end{aligned}$$

$Z_{matrix}([V]^{n+1})^{k+1} = [V^*]^n + ([\overline{\pi}]^{n+1})^k[\text{payoff}]^{n+1}$
if $max_i \frac{|((V_i)^{n+1})^{k+1} - ((V_i)^{n+1})^k|}{max(1, |((V_i)^{n+1})^{k+1}|)} < tol$
quit;
endfor; % end penalty American constration iteration
endfor; % end iteration along φ direction
$V(s_t, P_i, \varphi_{j+\Delta\tau}, \tau^n) = V^*(s_t)^n_{ij}$; % by linear interation
endfor; % end time step iteration

6.2.4 Properties of the numerical scheme

Since no closed-form solution exists for our optimal tree harvesting problem, the properties of our proposed numerical scheme have to been examined. In the case of nonlinear pricing problems, seemingly reasonable numerical schemes can converge to an incorrect solution[21]. A stable, consistent and monotone discretization will converge to the viscosity (i.e. correct) solution.[22]. Generally speaking, consistency is guaranteed if a reasonable discretization is used[23]. We use finite difference discretization which is a one of the standard discretization methods. In Appendix B, we prove that our scheme is monotone and stable and thus converges to the viscosity solution.

7 Optimal harvesting problem: data and empirical results

7.1 Cost, wood volume and price data

We examine an optimal harvesting problem for a hypothetical stand of Jack Pine trees in Ontario's boreal forest. We consider the optimal harvesting decision and land value assuming

[21]See Pooley et al. (2003).

[22]See Barles (1997) for detailed proof. For the definition of viscosity solution, see d'Halluin et al. (2005). For the existence of a viscosity solution in the regime switching case, see Pemy and Zhang (2006).

[23]See d'Halluin et al. (2005).

Item	Cost, $/ha	Age cost incurred
Site preparation	$200	1
Nursery stock	$360	1
Planting	$360	2
First tending	$120	5
Monitoring	$10	35

TABLE 6: *Silviculture costs under a basic regime*

Harvest and transportation cost	$47
Price of SPF1	$60
Price of SPF2	$55
Price of SPF3	$30
Price of poplar/birch	$20

TABLE 7: *Assumed values for log prices and cost of delivering logs to the mill in $ per cubic meter*

that the stand will continue to be used for commercial forestry operations over multiple rotations. Values are calculated prior to any stumpage payments or taxes.

Timber volumes and harvesting costs are adopted from Insley and Lei (2007) and are repeated here for the convenience of the reader. Volume and silviculture cost data were kindly provided by Tembec Inc. The estimated volumes reflect 'basic' levels of forestry management which involves $1040 per hectare spent within the first five years on site preparation, planting and tending. These costs are detailed in Table 6. Note that in the Canadian context these basic silviculture expenses are mandated by government regulation for certain stands.

Volumes, estimated by product, are shown in Figure 5 for the basic regime.[24] SPF1 and SPF2 are defined as being greater than 12 centimeters at the small end, SPF3 is less than 12 centimeters, and 'other' refers to other less valuable species (poplar and birch). Data used to plot this graph is provided in Insley and Wirjanto (2008).

Assumptions for harvesting costs and current log prices at the millgate are given in Table 7. These prices are considered representative for 2003 prices at the millgate in Ontario's boreal forest. Average cost to deliver logs to the lumber mill in 2003 are reported as $55 per cubic meter in a recent Ontario government report Ontario Ministry of Natural Resources (2005). From this is subtracted $8 per cubic meter as an average stumpage charge in 2003 giving $47 per cubic meter.[25] It will be noted the lower valued items (SPF3 and poplar/birch) are harvested at a loss. These items must be harvested according to Ontario government regulation. The price for poplar/birch is at roadside, so there is no transportation cost to the mill.

[24]The yield curves were estimated by Margaret Penner of Forest Analysis Ltd., Huntsville, Ontario for Tembec Inc and are available from the author on request.

[25]This consists of $35 per cubic meter for harvesting and $12 per cubic meter for transportation. Average stumpage charges are available from the Ontario Ministry of Natural Resources.

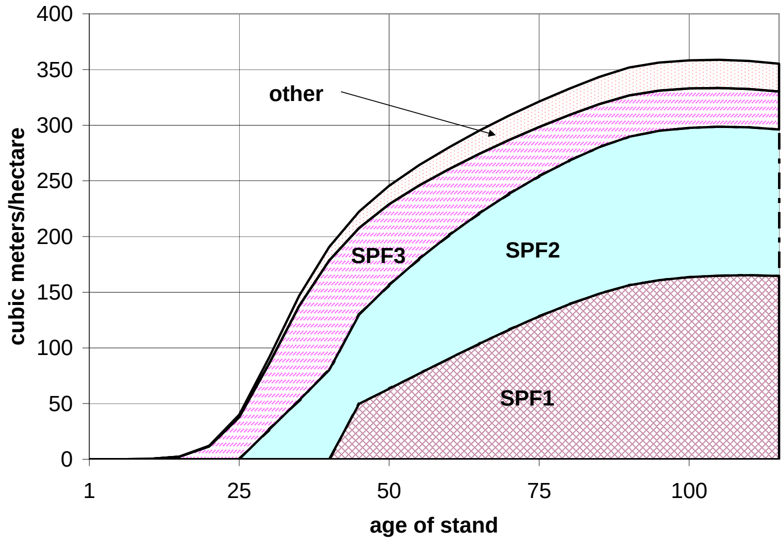

FIGURE 5: *Volumes by product for hypothetical Jack Pine stands in Ontario's boreal forest under basic management*

7.1.1 Results for land value and critical harvesting prices

The parameter values of the RSMR model used to evaluate the investment are provided in previous sections. The equilibrium price levels in the two regimes, $K(s_t)$, as shown in Table 2, are stated in Canadian dollars at Toronto. In order to value our hypothetical stand of trees, the equilibrium prices need to be scaled to reflect prices at the millgate. Our estimate of price at the millgate in 2003 for SPF1 logs is Cdn.\$60 per cubic meter. In 2003 the average spot price in Toronto was Cdn. \$375 per MBF. We use the ratio of 375/60 as adjustment factor to scale the equilibrium price levels. The scaled long-run price levels become $K(0) = \$11.51$ and $K(1) = \$82.66$ per cubic metre. This rescaling accounts for transportation costs from Toronto to the mill and milling costs (as well as the conversion from MBF to m^3).

Land values calculated using the RSMR and TMR models are provided in Table 8 for three different initial stand ages and two initial lumber prices. For the RSMR model, the value of the opportunity to harvest a stand at the beginning of rotation (stand age of zero) is \$2858 per hectare in either regime 1 or 2 regime and for both initial price levels shown. This reflects the fact that at the beginning of the rotation the harvest date is many years away and regime switching will likely happen numerous times over the next few decades. Hence the current regime has little effect on land value at the beginning of the rotation. Similarly the current price has a negligible effect on the value of the bare land. For older stands for which the optimal harvesting time is nearer, the value of the stand does depend positively on the current price of lumber. Further, the stand value is slightly higher in regime 1 than in

Land value in \$ per hectare, Initial lumber price of \$60/m^3			
	RSMR model		TMR model
Initial Stand age	Regime 0	Regime 1	Single regime
Age 0	2858	2858	1404
Age 50	10593	10728	5617
Age 75	13406	13660	9078
Land value in \$ per hectare, Initial lumber price of \$100/m^3			
	RSMR model		TMR model
Initial Stand age	Regime 0	Regime 1	Single regime
Age 0	2858	2858	1404
Age 50	11503	12242	7474
Age 75	15352	16619	13896

TABLE 8: *Land values at the beginning of the first rotation for regime switching and traditional mean reversion models, \$(2005)Canadian per hectare*

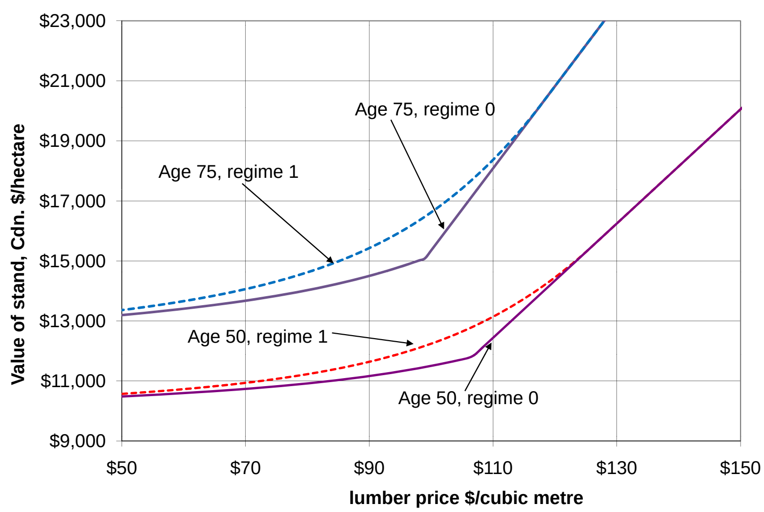

FIGURE 6: *Land values for different aged stands in the RSMR case. Dashed lines: Regime 1, solid lines: Regime 0*

regime 0. In Table 8, we observe that at an initial price of $\$100/m^3$ the land value in regime 1 is approximately 8% higher than in regime 0. Another perspective on land values for older stands is given in Figure 6. Here we see that land value for 50 and 75 year old stands rises with lumber price and that for a range of prices the value in regime 1 exceeds the value in regime 0. As will be seen below, this price range is around the critical price level that would trigger optimal harvesting.

The value of land in the TMR regime, also shown in Table 8, is $1404 per hectare at age 0, significantly lower than in the RSMR case. For comparison purposes we note that the land value for the same stand at age 0 calculated in Insley and Lei (2007) was $1630/ha. The analysis in Insley and Lei (2007) uses the same cost and yield data, with a TMR process. However the parameters of the TMR process were estimate through OLS on spot price data and the market price of risk was estimated separately.

Critical harvesting prices versus stand age are shown in Figure 7. For a stand of a given age, once the critical harvesting price is met or surpassed, harvesting of the stand and replanting for the next rotation are the optimal actions. Harvesting is not permitted in the model prior to age 35 until all silviculture expenditures have been made. Critical prices are high during the earlier ages when the trees are still growing, but fall as the stand ages and eventually reach a steady state. Critical prices are highest for Regime 1 which is characterized by a high equilibrium level and a slower speed of mean reversion. Higher prices are more likely in this regime, and it is worthwhile delaying harvesting until a higher threshold is reached. In contrast with regime 0 lower prices are more likely as the speed of mean reversion is faster and the equilibrium level is lower. Hence it is better to harvest at a lower threshold to avoid the possibility of facing an even lower price. Critical prices for the TMR case are consistently below those of the two regimes in the RSMR model.

In summary, although our calibration procedure was able to fit futures data quite well for both models, the RSMR price model results in significantly different land values and critical harvesting prices than the TMR model.

8 Concluding remarks

This paper investigates a possible improvement in the modelling of stochastic timber prices in optimal tree harvesting problems. Our goal is to find a modelling approach that is rich enough to capture the main characteristics of timber prices, while still being simple enough that the resulting price model can easily be incorporated into problems of forest investment valuation. We compare two different stochastic price process, a regime switching model with a different mean revering process in each regime (RSMR) and a traditional mean reverting model (TMR). The RSMR model allows for two states in lumber markets which we may characterize as being good times and bad times. The price models are calibrated using lumber futures prices and futures call option prices. The calibration process is able to find a reasonable fit for both models, but the mean absolute error is lower for the RSMR model.

In the second part of the paper, we use the calibrated timber price models in a real options model of the optimal harvesting decision. PDEs characterizing the value of the stand of trees are derived using contingent claim analysis. A linear complementarity problem (LCP) is then

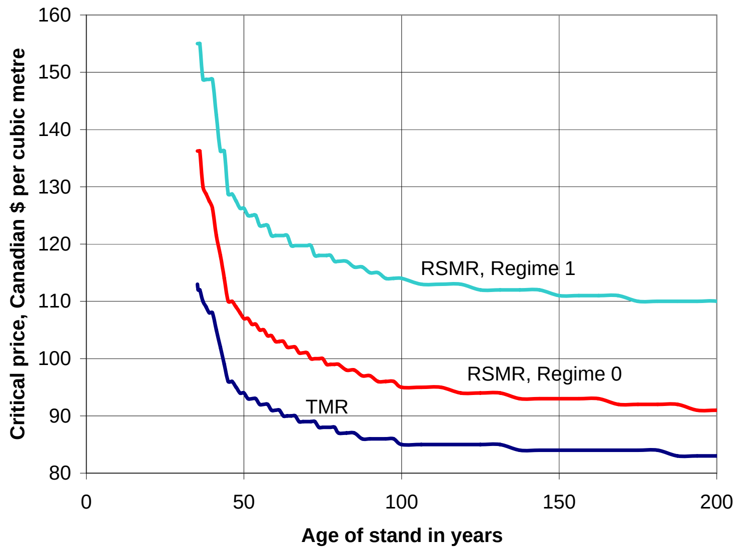

FIGURE 7: *Critical harvesting prices for the RSMR and TMR cases*

developed and solved using a fully implicit numerical method. We show that our numerical scheme converges to the viscosity solution (i.e. the correct solution.)

Our empirical example is for a hypothetical stand of trees in Ontario's boreal forest. For the RSMR model, the estimated land value at the beginning of the rotation is insensitive to the particular regime and at $2858 per hectare is of a reasonable order of magnitude. The land value for the TMR model is $1404 per hectare. We also examined critical harvesting prices, which for the RSMR model differ depending on the current regime.

We conclude that the RSMR model shows some promise as a parsimonious model of timber prices, that can fairly easily be incorporated into optimal harvesting models. One limitation of our methodology is in the use of short term maturity contracts in the calibration exercise. The longest maturity of the chosen futures contract is less than one year, but unfortunately this is all that is available. One may ask whether the calibrated parameter values are appropriate for long term forestry investment valuation problems. Schwartz and Smith (2000) has proposed a way of dealing with this issue. The applicability of his method for lumber prices is an area for future research.

Future research will also investigate the robustness of the RSMR model through comparison with other multi-factor models that have been used in the literature to value other commodity linked investments. We hope that other researchers will find the methodologies demonstrated here useful for the analysis of other types of investments, particularly those dependent on commodity prices where active futures markets exist.

References

Alvarez, L. H. and E. Koskela (2005). Wicksellian theory of forest rotation under interest rate variablity. *Journal of Economic Dynamics and Control 29*, 529–545.

Alvarez, L. H. and E. Koskela (2007). Taxation and rotation age under stochastic forest stand value. *Journal of Environmental Economics and Management 54*, 113–127.

Baker, M., S. Mayfild, and J. Parsons (1998). Alternative models of uncertain commodity prices for use with modern asset pricing methods. *19*, 115–148.

Barles, G. (1997). Convergence of numerical schemes for degenerate parabolic equations arising in finance. In L. Rogers and D. Talay (Eds.), *Numerical Methods in Finance*, pp. 1–21. Cambridge University Press.

Barz, G. and B. Johnson (May 1998). *Modeling the price of commodities that are costly to store: the case of electricity.* Chicago, IL.

Bessembinder, H., J. F. Coughenour, S. Paul, and M. M. Smoller (1995). Mean-reversion in equilibrium asset prices: Evidence from the futures term structure. *Journal of Finance 50*, 361–375.

Brazee, R. J., G. Amacher, and M. Conway (1999). Optimal harvesting with autocorrelated stumpage prices. *Journal of Forest Economics 5*, 193–200.

Caulfield, J. P. and D. H. Newman (1999). Dealing with timberland investment risk: Theory versus practice for institutional owners. *Journal of Forest Economics 5*, 253–268.

Chen, Z. and P. A. Forsyth (2008). Implications of a regime-switching model on natural gas storage valuation and optimal operation. *Quantitative Finance*. forthcoming.

Clarke, H. and W. Reed (1989). The tree-cutting problem in a stochastic environment. *Journal of Economic Dynamics and Control 13*, 569–95.

Cortazar, G. and E. S. Schwartz (1994). The valuation of commodity contingent claims. *Journal of Derivatives 1*, 27–39.

Davies, R. (1977). Hypothesis testing when a nuisance parameter is present only under the alternative. *Biometrika 64*, 247–254.

Davies, R. (1987). Hypothesis testing when a nuisance parameter is present only under the alternative. *Biometrika 74*, 33–43.

de Jong, C. (2005). The nature of power spikes: a regime-switching approach. Technical report, Rotterdam School of Management at Erasmus University.

Deng, S. (2000). Stochastic models of energy commodity prices and their applications: mean reversion with jumps and spikes. Technical report, University of California Energy Institute.

d'Halluin, Y., P. Forsyth, and G. Labahn (2005). A semi-lagrangian approach for american asian options under jump diffusion. *SIAM Journal on Scientific Computing 27*, 315–345.

Dixit, A. K. and R. S. Pindyck (1994). *Investment under uncertainty.* Princeton University Press, Princeton, NJ.

Fan, Q., P. Forsyth, J. McMacken, and W. Tang (1996). Performance issues for iterative solvers in device simulation. *SIAM Journal on Scientific and Statistical Computing 19*, 100–117.

Geman, H. (2005). *Commodities and commodity derivatives: Modelling and Pricing for Agriculturals, Metals and Energy.* John Wiley & Sons, Ltd, West Sussex, England.

Global Institute of Sustainable Forestry (2002). Institutional timberland investment. Technical Report 2, Yale Forest Forum, New Haven, Connecticut.

Gong, P. (1999). Optimal harvest policy with first-order autoregresive price process. *Journal of Forest Economics 5*, 413–439.

Hamilton, J. (1989). A new approach to the economic analysis of non-stationary time series and the business cycle. *Econometrica 57*, 357–384.

Hool, J. (1966). A dynamic programming-markov chain approach to forest production control. *Forestry Science Monograph 12*, 1–26.

Ikonen, S. and J. Toivanen (2008). Efficient numerical methods for pricing american options under stochastic volatility. *Numerical Methods for Partial Differential Equations 24*, 104–126.

Insley, M. and M. Lei (2007). Hedges and trees: Incorporating fire risk into optimal decisions in forestry using a no-arbritrage approach. *Journal of Agricultural and Resource Economics 32*, 492–514.

Insley, M. and K. Rollins (2005). On solving the multirotational timber harvesting problem with stochastic prices: a linear complemetarity formulation. *American Journal of Agricultural Economics 87*.

Insley, M. and T. Wirjanto (July 2008). Contrasting two approaches in real options valuation: contingetn claims versus dynamic programming.

Kaminski, V. (1997). *The US power market.* London: Risk Publications.

Lam, P. (1990). The hamilton model with a general autoregressive component. *Journal of Monetary Economics 26*, 409–432.

Lembersky, M. and K. Johnson (1975). Optimal policies for managed stands: an infinite horizon markov decision process approach. *Forest Science 21*, 109–22.

Lucia, J. and E. S. Schwartz (2002). Electricity prices and power derivatives:evidence from the nordic power exchange. *Review of Derivatives Research 5*, 5–50.

Morck, R., E. Schwartz, and D. Strangeland (1989). The valuation of forestry resources under stochastic prices and inventories. *Journal of Financial and Quantitative Analysis 4*, 473–487.

Morton, K. and D. Mayers (1994). *Numerical solution of partial differential equations).* Cambridge University Press, Cambridge.

Ontario Ministry of Natural Resources (May, 2005). Minister's Council on Forest Sector Competitivenes, Final Report.

Pemy, M. and Q. Zhang (2006). Optimal stock liquidation in a regime switching model with finite time horizon. *Journal of Mathematical Analysis and Applications 321*, 537–552.

Pilipovic, D. (2007). *Energy risk: valuing and managing energy derivatives, second edition.* McGraw-Hill, New York.

Plantinga, A. J. (1998). The optimal timber rotation: An option value approach. *Forest Science 44*, 192–202.

Pooley, D., P. Forsyth, and K. Vetzal (2003). Numerical convergence properties of option pricing pdes with uncertain volatility. *IMA Journal of Numerical Analysis 23*, 241–267.

Raymond, J. and R. Rich (1997). Oil and the macroeconomy: a markov state-switching approach. *Journal of Money, Credit and Banking 29.*

Reed, W. and H. Clarke (1990). Harvest decisions and asset valuation for biological resources exhibiting size-dependent stochastic growth. *International Economic Review 31*, 147–169.

Saphores, J.-D., L. Khalaf, and D. Pelletier (2002). On jump and arch effects in natural resource prices: An application to pacific northwest stumpage prices. *American Journal of Agricultural Economics 84*, 387–400.

Schwartz, E. (1997). The stochastic behavior of commodity prices: implications for valuation and hedging. *Journal of Finance 52*, 923–973.

Schwartz, E. and J. E. Smith (2000). Short-term variations and long-term dynamics in commodity prices. *Management Science 46*, 893–911.

Schwert, G. W. (1996). Markup pricing in mergers and acquisitions. *Journal of Financial Economics 41*, 153–192.

Smith, J. E. and K. F. McCardle (1998). Valuing oil properties: Integration option pricing and decision analysis approaches. *Operation Research 46*, 198–217.

Thomson, T. (1992). Optimal forest rotation when stumpage prices follow a diffusion process. *Land Economics 68*, 329–342.

Varga, R. (2000). *Matrix iterative analysis.* Springer, New York.

Yin, R. and D. Newman (1995). A note on the tree-cutting problem in a stochastic environment. *Journal of Forest Economics 1:2*.

Yin, R. and D. Newman (1997). When to cut a stand of trees. *Natural Resource Modeling 10*, 251–61.

Zvan, R., P. Forsyth, and K. Vezal (1998). A penalty method for american options with stochastic volatility. *Journal of Computational and Applied Mathematics 91*, 199–218.

Appendix

A Numerical solution of LCP

The basic linear complementarity problem of our optimal tree harvesting problem can be expressed as Equation (32)

$$V(s_t)_\tau - V(s_t)_\alpha = \alpha(s_t)(K(s_t) - P)V(s_t)_P + \frac{1}{2}(\sigma(s_t)P)^2 V(s_t)_{PP} - rV(s_t) + \lambda^{s_t \to 1-s_t}(V(1-s_t) - V(s_t)) + \Upsilon(s_t) \quad \text{(A1)}$$

This PDE is discretized using unequally spaced grids in the directions of P and α. Time direction is also discretized. Define nodes on the axes for P, α and τ by

$$\begin{aligned} P &= [P_1, P_2, ..., P_I] \quad \text{(A2)} \\ \alpha &= [\alpha_1, \alpha_2, ..., \alpha_J] \\ \tau &= [\tau_1, \tau_2, ..., \tau_N] \end{aligned}$$

Using fully implicit difference method, the difference scheme for Equation (A1) can be written as

$$\frac{V(s_t, P_i, \alpha_j, \tau^{n+1}) - V(s_t, P_i, \alpha_{j+\Delta\tau}, \tau^n)}{\Delta\tau} = \Big[\alpha(s_t)(K(s_t) - P)V(s_t)_P + \frac{1}{2}(\sigma(s_t)P)^2 V(s_t)_{PP} - rV(s_t) + \lambda^{s_t \to 1-s_t}(V(1-s_t) - V(s_t)) + \Upsilon(s_t)\Big]_{ij}^{n+1} \quad \text{(A3)}$$

For simplicity, define $V(s_t)_{ij}^{n+1} = V(s_t, P_i, \alpha_j, \tau^{n+1})$, $V^*(s_t)_{ij}^n = V(s_t, P_i, \alpha_{j+\Delta\tau}, \tau^n)$ and rewrite Equation (A3) as

$$\frac{V(s_t)_{ij}^{n+1} - V^*(s_t)_{ij}^n}{\Delta\tau} = \Big[\alpha(s_t)(K(s_t) - P)V(s_t)_P + \frac{1}{2}(\sigma(s_t)P)^2 V(s_t)_{PP} - rV(s_t) + \lambda^{s_t \to 1-s_t}(V(1-s_t) - V(s_t)) + \Upsilon(s_t)\Big]_{ij}^{n+1} \quad \text{(A4)}$$

Since the right hand side of Equation (A4) only contains the state variable P, this one-dimensional PDE is solved numerically for each stand age α_j within each time step. After one time step iteration completes, using linear interpolation to get $V(s_t, P_i, \alpha_{j+\Delta\tau}, \tau^n)$. Hence our only concern is the discretization of derivatives with respect to P.

A1 Discretization for interior points along P direction

For simplicity, the dependence of the regime s_t is dropped for discretization, except for $V(1-s_t)$ in Equation (A4). Hence it can be further simplified as

$$\frac{V_{ij}^{n+1}-V_{ij}^{*n}}{\Delta\tau} = \left[\alpha(K-P)V_P + \frac{1}{2}(\sigma P)^2 V_{PP} - rV + \lambda^{s_t\to 1-s_t}(V(1-s_t)-V) + \Upsilon\right]_{ij}^{n+1} \quad \text{(A5)}$$

Central difference, forward difference and backward difference methods can be used to discretize the first derivative term V_P for interior points $i=[2,...,I-1]$. We choose the difference method which will assure the positive coefficient scheme. If all these three methods can guarantee the positive coefficient scheme, central difference will be picked up for its faster convergence. For illustration purpose, the complete discretiztion equation will use central difference method for V_P.

$$\begin{aligned}\frac{V_{ij}^{n+1}-V_{ij}^{*n}}{\Delta\tau} = & \left\{\frac{\sigma^2P^2}{2}\left[\frac{\frac{V_{i+1,j}-V_{ij}}{P_{i+1}-P_i}-\frac{V_{ij}-V_{i-1,j}}{P_i-P_{i-1}}}{\frac{P_{i+1}-P_{i-1}}{2}}\right] + \alpha(K-P)\left[\frac{V_{i+1,j}-V_{i-1,j}}{P_{i+1}-P_{i-1}}\right]\right. \\ & \left. -(r+\lambda^{s_t\to 1-s_t})V_{ij} + \lambda^{s_t\to 1-s_t}V(1-s_t)_{ij} + \frac{\overline{\pi_{ij}}}{\Delta\tau}[(P_i-C)Q_j + V_{i0} - V_{ij}]\right\}^{n+1} \quad \text{(A6)}\end{aligned}$$

Equation (A6) can be simplified as

$$\begin{aligned}\frac{V_{ij}^{n+1}-V_{ij}^{*n}}{\Delta\tau} &= a_iV_{i-1,j}^{n+1} + b_iV_{i+1,j}^{n+1} - [a_i + b_i + r + \lambda^{s_t\to 1-s_t} + \frac{\overline{\pi_{ij}}}{\Delta\tau}]V_{ij}^{n+1} \\ &+ \lambda^{s_t\to 1-s_t}V(1-s_t)_{ij}^{n+1} + \frac{\overline{\pi_{ij}}}{\Delta\tau}[(P_i-C)Q_j + V_{i0} - V_{ij}^{n+1}] \quad \text{(A7)}\end{aligned}$$

where define $\alpha_i \equiv \frac{\sigma^2P_i^2}{P_{i+1}-P_{i-1}}$

1. **For central difference method**

$$a_i \equiv \frac{\alpha_i}{P_i-P_{i-1}} - \frac{\alpha(K-P_i)}{P_{i+1}-P_{i-1}}; \qquad b_i \equiv \frac{\alpha_i}{P_{i+1}-P_i} + \frac{\alpha(K-P_i)}{P_{i+1}-P_{i-1}}$$

2. **For forward difference method**

$$a_i \equiv \frac{\alpha_i}{P_i-P_{i-1}}; \qquad b_i \equiv \frac{\alpha_i}{P_{i+1}-P_i} + \frac{\alpha(K-P_i)}{P_{i+1}-P_i}$$

3. **For backward difference method**

$$a_i \equiv \frac{\alpha_i}{P_i-P_{i-1}} - \frac{\alpha(K-P_i)}{P_i-P_{i-1}}; \qquad b_i \equiv \frac{\alpha_i}{P_{i+1}-P_i}$$

A2 Discretization of boundary conditions for $i = 1$ and $i = I$

When $P = 0$, no specific boundary condition is needed. Substitute $P = 0$ into LCP Equation (A1) to get PDE for this boundary

$$V(s_t)_\tau - V(s_t)_\varphi = \alpha(s_t)K(s_t)V(s_t)_P - rV(s_t) + \lambda^{s_t \to 1-s_t}(V(1-s_t) - V(s_t)) + \Upsilon(s_t) \quad (A8)$$

Using forward discretization for $V(s_t)_P$, the discrete version of Equation (A8) can be written as

$$\frac{V_{1j}^{n+1} - V_{1j}^{*n}}{\Delta\tau} = b_1 V_{2,j}^{n+1} - [b_1 + r + \lambda^{s_t \to 1-s_t} + \frac{\overline{\pi_{1j}}}{\Delta\tau}]V_{1j}^{n+1} + \lambda^{s_t \to 1-s_t} V(1-s_t)_{1j}^{n+1} + \frac{\overline{\pi_{1j}}}{\Delta\tau}[(P_1 - C)Q_j + V_{10} - V_{1j}^{n+1}] \quad (A9)$$

where $b_1 = \frac{\alpha K}{P_1 - P_0}$.

When $P = P_I$, the option value is a linear function of the price. Hence the second derivative term $V(s_t)_{PP} = 0$. Guess the solution $V(s_t)_{Ij} = A(\tau) + B(\tau)P_I$. When $P \to \infty$, the term $B(\tau)P_I$ dominates and $V(s_t)_{Ij} \approx B(\tau)P_I$. For the first derivative term $\alpha(s_t)(K(s_t) - P)V(s_t)_P$, $P_I \gg K(s_t)$. Hence $\alpha(s_t)(K(s_t) - P)V(s_t)_P \approx -\alpha(s_t)PV(s_t)_P = -\alpha(s_t)V(s_t)$. The LCP equation (A1) in this boundary can then be expressed as

$$V(s_t)_\tau - V(s_t)_\varphi = -\alpha(s_t)V(s_t) - rV(s_t) + \lambda^{s_t \to 1-s_t}(V(1-s_t) - V(s_t)) + \Upsilon(s_t) \quad (A10)$$

The discrete version of Equation (A10) can be written as

$$\frac{V_{Ij}^{n+1} - V_{Ij}^{*n}}{\Delta\tau} = -[\alpha + r + \lambda^{s_t \to 1-s_t} + \frac{\overline{\pi_{Ij}}}{\Delta\tau}]V_{Ij}^{n+1} + \lambda^{s_t \to 1-s_t} V(1-s_t)_{Ij}^{n+1} + \frac{\overline{\pi_{Ij}}}{\Delta\tau}[(P_I - C)Q_j + V_{I0} - V_{Ij}^{n+1}] \quad (A11)$$

A3 Complete discretization

Combine Equations (A7), (A9) and (A11), and write them in matrix form as

$$[(1 + \Delta\tau(r + \lambda^{s_t \to 1-s_t}))I + W(s_t) + \overline{\pi}^{n+1}]V(s_t)^{n+1} - \Delta\tau\lambda^{s_t \to 1-s_t}V(1-s_t)^{n+1} = V(s_t)^{*n} + \overline{\pi(s_t)}^{n+1}[(P - C)Q + V(s_t)_0^{n+1}] \quad (A12)$$

where $W(s_t)$ is a square sparse matrix which has the following elements:

$$W(s_t) = \begin{bmatrix} \Delta\tau b_1 & -\Delta\tau b_1 & 0 & 0 & 0 & ... & 0 & 0 \\ -\Delta\tau a_2 & \Delta\tau(a_2 + b_2) & -\Delta\tau b_2 & 0 & 0 & ... & 0 & 0 \\ ... & ... & ... & ... & ... & ... & ... & ... \\ 0 & 0 & 0 & ... & 0 & -\Delta\tau a_{I-1} & \Delta\tau(b_{I-1} + b_{I-1}) & -\Delta\tau a_{I-1} \\ 0 & 0 & 0 & ... & 0 & 0 & 0 & \Delta\tau\alpha(s_t) \end{bmatrix} \quad (A13)$$

The above analysis for the option value in regime s_t can be used in the same way for the option value in the other regime $1-s_t$. The similar equation as Equation (A12) can be derived for $V(1-s_t)$ which can be written as

$$[(1+\Delta\tau(r+\lambda^{1-s_t\to s_t}))I+W(1-s_t)+\overline{\pi}^{n+1}]V(1-s_t)^{n+1}-\Delta\tau\lambda^{1-s_t\to s_t}V(s_t)^{n+1}= V(1-s_t)^{*n}+\overline{\pi(1-s_t)}^{n+1}[(P-C)Q+V(1-s_t)_0^{n+1}] \quad \text{(A14)}$$

Denote $AA(s_t)=[(1+\Delta\tau(r+\lambda^{s_t\to 1-s_t}))I+W(s_t)+\overline{\pi}^{n+1}]$. Then its counterpart for regime $1-s_t$ can be defined as $AA(1-s_t)=[(1+\Delta\tau(r+\lambda^{1-s_t\to s_t}))I+W(1-s_t)+\overline{\pi}^{n+1}]$. Stack Equations (A12) and (A14) together and get

$$\begin{bmatrix} AA(s_t) & -\Delta\tau\lambda^{s_t\to 1-s_t} \\ -\Delta\tau\lambda^{1-s_t\to s_t} & AA(1-s_t)\end{bmatrix}\begin{bmatrix} V(s_t) \\ V(1-s_t)\end{bmatrix}^{n+1}=\begin{bmatrix} V^*(s_t) \\ V^*(1-s_t)\end{bmatrix}^{n}+ \begin{bmatrix} \overline{\pi(s_t)} \\ \overline{\pi(1-s_t)}\end{bmatrix}^{n+1}\begin{bmatrix} payoff(s_t) \\ payoff(1-s_t)\end{bmatrix}^{n+1} \quad \text{(A15)}$$

where $Z_{matrix}=\begin{bmatrix} AA(s_t) & -\Delta\tau\lambda^{s_t\to 1-s_t} \\ -\Delta\tau\lambda^{1-s_t\to s_t} & AA(1-s_t)\end{bmatrix}$.

B Convergence to the viscosity solution

In this appendix, the monotonicity and stability properties of the discrete equations in our numerical scheme are analyzed. We claimed earlier that our scheme is consistent. A discretization that is consistent, monotone, and stable will converge to the viscosity solution.

Before proving the monotonicity and stability of our scheme, it is useful to gather together several results for the finite difference discretization.

Lemma B.1. *Z_{matrix} is an M matrix*[26]

Proof. Equation (35) is discretized using central difference, forward difference or backward difference methods to get a positive coefficient discretizations. The positive coefficient discretization means that Z_{matrix} has non-positive offdiagonal elements. Moreover, the sum of all elements in each row of Z_{matrix} is non-negative[27]. Hence Z_{matrix} is an M matrix. □

We follow d'Halluin et al. (2005)'s definition of monotone discretizations and rewrite the discrete Equation (32) at each pair of node (P_i,φ_j) as[28]

$$\begin{aligned} g_{ij}(V_{ij}^{n+1},\{V_{i^-j}^{n+1}\},\{V^n\}) &= -[ZV_j^{n+1}]_i+[\Phi^{n+1}V^n]_{ij}+[\overline{\pi}^{n+1}]_{ii}(\text{payoff}_{ij}-V_{ij}^{n+1}) \\ &= 0 \end{aligned} \quad \text{(B1)}$$

where $\{V_{i^-,j}^{n+1}\}$ denotes the set of values $V_{i^-,j}^{n+1}$ without the ith element V_{ij}^{n+1}. Φ^{n+1} in this expression is the Lagrange linear interpolant operator[29] used to deal with linear interpolation in the semi-lagrangian method.

$$[\Phi^{n+1}V^n]_{ij}=V(s_t,P_i,\varphi_{j+\Delta\tau},\tau^n)+\text{ interpolation error}$$

[26] For definition and properties of M matrix, see Varga (2000).

[27] This can be checked from detailed discretization in Appendix A.

[28] For simplicity, in this expression $V\equiv V(s_t)$ or $V\equiv V(1-s_t)$.

[29] For details about Lagrange linear interpolation operator, see d'Halluin et al. (2005).

Theorem B.2. *The discretization scheme* (B1) *is unconditionally monotone.*

Proof. In Lemma B.1 we have already showed that Z is an M-matrix. Therefore, $-[ZV_j^{n+1}]_i$ is a strictly decreasing function of V_{ij}^{n+1}, and a non-decreasing function of $\{V_{i^-,j}^{n+1}\}$. $[\Phi^{n+1}V^n]_{ij}$ is a non-decreasing function of $\{V^n\}$, since Φ^{n+1} is a linear interpolant operator. The last term in equation (B1) $[\overline{\pi}^{n+1}]_{ii}(payoff_{ij} - V_{ij}^{n+1})$ is a non-increasing function of V_{ij}^{n+1} since the elements in $[\overline{\pi}^{n+1}]_{ii}$ are non-negative. Therefore, this discretization scheme is monotone based on d'Halluin et al. (2005)'s definition. □

Theorem B.3. *The scheme satisfies*

$$||V^{n+1}||_\infty \leq \max\{||V^n||_\infty, ||payoff||_\infty\}$$

and is unconditionally stable.

Proof. Write out the complete discretized version of Equation (32) as

$$-\Delta\tau V(s_t)_{i-1,j}^{n+1} + [1 + \Delta\tau(a(s_t)_i + b(s_t)_i + r + \lambda^{k\to 1-k}) + \overline{\pi(s_t)_{ij}^{n+1}}]V(s_t)_{ij}^{n+1} - \Delta\tau b(s_t)_i V(s_t)_{i+1,j}^{n+1}$$
$$-\Delta\tau\lambda^{k\to 1-k}V(1-s_t)_{ij}^{n+1} = \sum_{ij} w_{ij}V(s_t)_{ij}^n + \overline{\pi(s_t)_{ij}^{n+1}}\,payoff_{ij} \quad \text{(B2)}$$

where w_{ij} is linear interpolant weight, satisfying $0 \leq w_{ij} \leq 1$ and $\sum w_{ij} = 1$. $a(s_t)_i$ and $b(s_t)_i$[30] are the components in Z matrix, which are non-negative. Denote $|V(s_t)_{m,j}^{n+1}| = ||V_j^{n+1}||_\infty$ where m is an index. Equation (B2) implies that

$$||V_j^{n+1}||_\infty(1 + r\Delta\tau + \overline{\pi}_{mm}) \leq ||V^n||_\infty + \overline{\pi}_{mm}||\text{payoff}||$$

which can be further simplified as

$$||V_j^{n+1}||_\infty(1 + r\Delta\tau + \overline{\pi}_{mm}) \leq \max\{||V^n||_\infty, ||payoff||_\infty\}(1 + \overline{\pi}_{mm}) \quad \text{(B3)}$$

Rearrange Equation (B3)

$$||V_j^{n+1}||_\infty \leq \max\{||V^n||_\infty, ||payoff||_\infty\}\frac{(1 + \overline{\pi}_{mm})}{(1 + r\Delta\tau + \overline{\pi}_{mm})}$$

Hence just as claimed, we get

$$||V^{n+1}||_\infty \leq \max\{||V^n||_\infty, ||payoff||_\infty\}$$

and the scheme is unconditionally stable

□

[30]The detailed expression is in Appendix A.